Doctorate Dissertation

博士論文

Developmental genetic studies on spikelet formation in *Oryza sativa*

（イネの小穂形成に関する発生遺伝学的研究）

A Dissertation Submitted for Degree of Doctor of Philosophy

December 2018

平成 30 年 12 月博士（理学）申請

Department of Biological Sciences, Graduate School of Science,

The University of Tokyo

東京大学大学院理学系研究科生物科学専攻

Shigehiro Sugiyama

杉山　茂大

Contents

Acknowledgements 1

List of abbreviations 2

Abstract 4

Chapter 1 General introduction

General introduction **7**

Figures 11

Chapter 2 Analysis of the mechanisms underlying carpel specification and flower meristem determinacy in rice

Introduction 12

Results 17

Discussion 27

Figures 36

Chapter 3 Morphological analysis of *tol* mutant which shows pleiotropic phenotypes in both spikelet and flower organs

Introduction 46

Results 50

Discussion 59

Tables 65

Figures 68

Chapter 4 Materials and methods

Materials and methods 75

Tables 79

Chapter 5 Conclusion and perspective

Conclusion and perspective 80

References 83

Acknowledgements

First of all, I would like to express my sincerest appreciation to Prof. Hiro-Yuki Hirano for giving me the opportunity to do my dissertation work in his laboratory and for supervising and encouraging me throughout this study. I am also most deeply grateful to Professors Mitsutomo Abe, Ichiro Terashima, Kyoko Ohashi-Ito and Takeshi Izawa (Graduate School of Agricultural and Life Sciences) for their critical and valuable suggestions to complete my thesis.

I would like to thank all lab members of the Laboratory of Evolutionary Genetics (The University of Tokyo) for encouragement and discussion. I especially thank Dr. Wakana Tanaka for her kind supports and discussion, Dr. Yukiko Yasui for the preparation of mutant lines and kind supports and Ms. Suzuha Ohmori for the permission to use her in situ datum.

I wish to thank to Dr. Masaki Endo (Yokohama City University) for kindly providing the pZH_OsU3gYSA_MMCas9 and pU6gRNA-oligo vector, Drs. Akio Miyao and Hirohiko Hirochika (NIAS) for providing *tol* and three mutant lines of *RLA1*, Drs. Tetsuya Kurata and Tomoaki Sakamoto (NAIST) for the next generation sequencing, Dr. Martin Kater (Universita` degli Studi di Milano) for providing a mutant line of *OsMADS58*, Dr. Ken-Ichi Nonomura and Mr. Mitsugu Eiguchi (National Institute of Genetics) and technicians at the Institute for Sustainable Agro-ecosystem Services of the University of Tokyo for cultivating rice used in my study.

Lastly, I would like to thank my family for their continuous supports.

List of abbreviations

ACS	acyl-CoA synthetase
AG	*AGAMOUS*
AP2	*APETALA2*
AP3	*APETALA3*
CLV	*CLAVATA*
CYC	*CYCLOIDEA*
CRC	*CRABS CLOW*
CRISPR/Cas9	clustered regularly interspaced short palindromic repeats/CRISPR-associated protein 9
DL	*DROOPING LEAF*
DP1	*DEPRESSED PALEA1*
G1	*LONG STERILE LEMMA1*
FON1	*FLORAL ORGAN NUMBER1*
FON2	*FLORAL ORGAN NUMBER2*
gRNA	guide RNA
KNU	*KNUCKLES*
LACS	long chain acyl-CoA synthetase
LCFA	long chain fatty acids
ONI1	*ONION1*
ONI2	*ONION2*

PI	*PISTILLATA*
PLE	*PLENA*
RLA1	*RICE LACS1*
SEM	scanning electron microscopy
SHP1	*SHATTER PROOF1*
SHP2	*SHATTER PROOF2*
SPW1	*SUPERWOMAN1*
STK	*STICKSEED*
T65	Taichung65
TH1	*TRIANGULAR HULL1*
TILLING	targeting induced local lesions in genomes
tol	*two opposite lemma*
VLCFA	very long chain fatty acids
WUS	*WUSCHEL*

Abstract

Elucidation of the molecular mechanisms underlying flower and inflorescence development is one of the central issues in plant developmental biology. Although angiosperms produce diverse flowers, the basic mechanisms of their development, represented by the ABC model, are conserved. Rice (*Oryza sativa*), a model monocot, has unique inflorescence unit, spikelet, in which flower is formed. Although ABC model is basically conserved in rice, further studies are necessary to explain the mechanism of rice flower development. In addition, the mechanisms of the formation of the organs specific to the spikelet have not yet fully explained so far.

In this thesis, firstly, I focused on carpel specification and flower meristem determinacy in rice. I revealed that class C MADS-box genes are not a key regulator for carpel specification and that the *DROOPING LEAF* (*DL*) gene plays a crucial function in regulating the determinacy of the flower meristem in addition to the class C genes. Secondly, I investigated the *two opposite lemma* (*tol*) mutant, which showed the pleiotropic phenotypes in both spikelet and flower organs. I identified *RICE LACS1* (*RLA1*) as the gene partially responsible for *tol* phenotype.

Mechanisms of the carpel specification and flower meristem determinacy

My laboratory previously reported that carpels are specified by the *YABBY* gene *DROOPING LEAF* (*DL*) in rice (*Oryza sativa*), which bears flowers that are distinct from those of eudicots. By contrast, another group reported that carpels are specified by

two class C genes, *OsMADS3* and *OsMADS58*.

Here, I have addressed this controversial issue by phenotypic characterization of floral homeotic gene mutants. Analysis of a complete loss-of-function mutant of *OsMADS3* and *OsMADS58* revealed that carpel-like organs expressing *DL* were formed in the absence of the two class C genes. Furthermore, no known flower organs including carpels were specified in a double mutant of *DL* and *SUPERWOMAN1* (a class B gene), which expresses only class C genes in whorls 3 and 4. Taken together with the analyses of the expression patterns of maker genes for each floral organ, these results clearly indicated that, in contrast to *Arabidopsis thaliana*, class C genes are not a key regulator for carpel specification in rice. Instead, they seem to be involved in the elaboration of carpel morphology rather than its specification. The major function of class C genes are likely to regulate the determinacy of the flower meristem. My phenotypic analysis also revealed that, similar to its *Arabidopsis* ortholog *CRABS CLAW*, *DL* plays an important function in regulating flower meristem determinacy in addition to carpel specification.

Analysis of the *tol* mutant that shows pleiotropic phenotypes in spikelets and flowers

Bilaterally symmetric flowers have evolved multiple times in different angiosperm lineages from radially symmetric ancestors. In contrast to *Arabidopsis*, grasses such as rice (*Oryza sativa*) and maize (*Zea mays*) generate bilaterally symmetric flowers and spikelets.

I focused on the *two opposite lemma* (*tol*) mutant in rice, which displays a

pleiotropic phenotype in the spikelet. Close morphological examination revealed that a typical spikelet phenotype of the *tol* mutant was principally based on the mirror image duplication of the lemma-side half of the spikelet, suggesting the disruption of the polarity along the lemma-palea axis. The observation of developing spikelets at early stages suggested that the *tol* phenotypes are caused by defects in the regulation of the size and activity of the flower meristem.

I revealed that the *RICE LACS1* (*RLA1*) gene, which catalyze the synthesis of very long chain fatty acids (VLCFA), was partially responsible for *tol* phenotype, suggesting that VLCFA is involved in *tol* phenotype. However, my analysis raised a possibility that the *tol* mutant was caused by double mutations, that is, the mutation in *RLA1* and that occurring in an unknown gene.

Chapter 1

General introduction

Mechanisms of flower development

Elucidation of the molecular mechanisms underlying flower and inflorescence development is one of the central issues in plant developmental biology. In *Arabidopsis thaliana*, the model plant of eudicots, the flower consists of four types of organs formed in the concentric arrangement: sepals are formed in whorl 1, petals in whorl 2, stamens in whorl 3 and carpels in whorl 4. This flower structure is basically common to most of angiosperms.

The ABC model that explains the principle of floral organ specification is a great milestone in flower development research (reviewed in Coen and Meyerowitz, 1991; Lohmann and Weigel, 2002; Prunet and Jack, 2014). In the ABC model, the flower organ identity is specified by sole or combinational activities of the genes classified into class A, B and C: the class A genes specify sepal identity, A and B petal identity, B and C stamen identity and C alone carpel identity. A large number of studies to understand further the detailed mechanisms of flower development have been performed based on this model in *Arabidopsis* (reviewed in Coen and Meyerowitz, 1991; Lohmann and Weigel, 2002; Prunet and Jack, 2014). ABC genes encode MASD domain transcription factor except for *APETELA2*. Developmental genetic studies in other plants have revealed that the ABC model is applicable in principle to not only

eudicot flowers but also monocot flowers, although floral shapes are diversified across angiosperms.

The mechanisms of spikelet development in rice

The molecular mechanisms of flower development are relatively well understood in rice among monocots, (reviewed in Hirano et al., 2014; Tanaka et al., 2014; Yoshida and Nagato, 2011). In grasses, floral organs are formed in a unique inflorescence unit, the spikelet. The spikelet consists of floral organs such as lodicules (petal homolog), stamens and carpels, and of organs specific to the spikelets such as a lemma, a palea, sterile lemmas and rudimentary glumes (Fig. 1-1). In rice flower, the carpel is located at the center of the flower (whorl 4), six stamens surround carpel (whorl 3) and two lodicules are formed asymmetrically on the lemma side (whorl 2) (Fig. 1-1B). These flower organs were enclosed by a lemma and a palea. Outside the lemma and palea, there are two sterile lemmas and two rudimentary glumes.

The ABC model is basically applicable to rice flower development. Class B genes such as *SUPERWOMAN1* (*SPW1;* also known as *OsMADS16*), *OsMADS2* and *OsMADS4* specify stamen and lodicule identity together with class C and class A genes, respectively (Nagasawa et al., 2003; Yao et al., 2008). Because the lodicule is a homolog of the petal in eudicots, the function of class B genes are conserved in rice and *Arabidopsis*. Similarly, class A gene such as *OsMADS14* is involved in lodicule specification (Wu et al., 2017). However, the mechanism of carpel specification differs between rice and *Arabidopsis*. In rice, the *YABBY* gene *DROOPING LEAF* (*DL*), which

is not included in the ABC model, plays a crucial role in carpel specification in rice (Nagasawa et al., 2003; Yamaguchi et al., 2004), whereas the class C gene *AGAMOUS* (*AG*) specifies in *Arabidopsis*. As for class C gene in rice, my laboratory revealed that the class C genes, *OsMADS3* and *OsMADS58*, are not involved in carpel specification (Yamaguchi et al., 2004). By contrast, another group reported that the carpel is specified by the class C genes (Dreni et al., 2011). Thus, the mechanisms of carpel specification and the actual role of class C genes are controversial in rice flower development.

As described above, rice has the unique inflorescence unit, the spikelet. Class A genes, *OsMADS14* and *OsMADS15*, are involved in lemma and palea development (Wu et al., 2017). *LONG STERILE LEMMA1* (*G1*), which encodes the protein with ALOG domain, specifies sterile lemma identity, and *g1* mutant showed the homeotic transformation of sterile lemmas into lemma (Yoshida et al., 2009). Although these studies have promoted the understanding of the mechanisms underlying spikelet development in rice, current understanding is insufficient to fully explain spikelet development.

Composition of this thesis

In this thesis, I attempted to understand the genetic mechanisms underlying the spikelet and flower development in rice through two independent approaches.

In chapter 2, I focused on carpel specification and flower meristem determinacy in rice. As described above, the functions of rice class C genes are controversial. By detailed phenotypic analyses of combination of several floral

homeotic mutants, I concluded that class C genes are not a key regulator for carpel specification in rice. In addition, I revealed that *DL* plays a crucial function in regulating the determinacy of the flower meristem.

In chapter 3, I investigated the *two opposite lemma* (*tol*) mutant, which showed the pleiotropic phenotypes in both spikelet and flower organs. The results suggest that the pleiotropic phenotypes are associated with an enlargement of the flower meristem together with partial failure in its maintenance. Identification of the gene partially responsible for the *tol* mutation suggest that the synthesis of very long chain fatty acid (VLCFA) is important for normal spikelet development in rice.

In chapter 4, I describe the plant materials and methods, which is used in my analysis.

In chapter 5, I conclude my investigations and discuss the perspective.

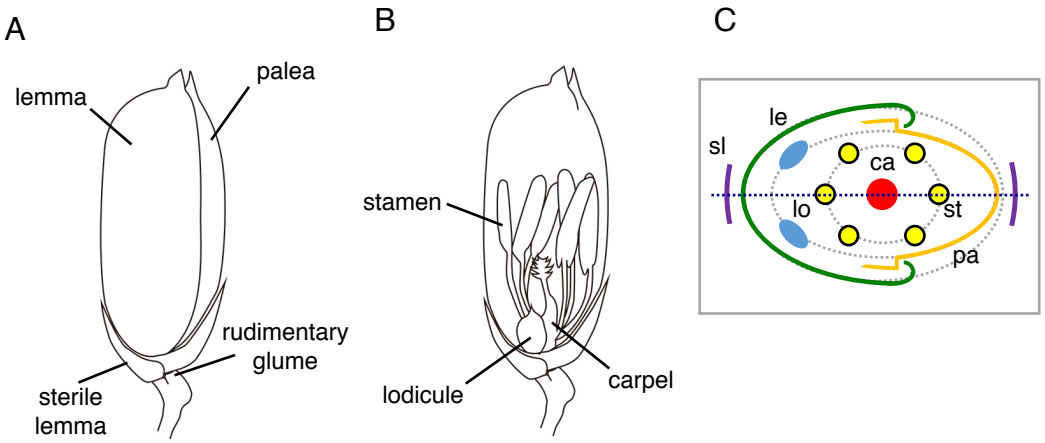

Fig. 1-1 Spikelet structure in rice.
(A, B) Illustrations of rice spikelet (A) and flower (B).
(C) Schematic representation of the rice spikelet. Green and orange indicate the lemma and the palea, respectively. The horizontal broken line indicates a plane of symmetry. Gray broken lines indicate concentric whorls.
ca, carpel; le, lemma; lo, lodicule; pa, palea; sl, sterile lemma; st, stamen.

Chapter 2

Introduction

Angiosperms generate a wide range of diverse flowers. Despite this diversity, the genetic mechanism underlying flower development is thought to be conserved among flowering plants and is represented by the ABC model, a milestone of plant developmental studies (reviewed in Coen and Meyerowitz, 1991). The premise of the ABC model is that each type of flower organ, including sepal, petal, stamen, and carpel, is specified by individual or combinatorial activity of floral homeotic genes, classified as A, B, and C genes (Bowman et al., 1991; reviewed in Coen and Meyerowitz, 1991; Jack, 2004; Lohmann and Weigel, 2002). The model was originally based on genetic studies using two model eudicots, *Arabidopsis thaliana* and *Antirrhinum majus*; however, the framework of the ABC model has been shown to be widely applicable to angiosperms, including grass species that produce flowers that are distinct from eudicots.

Among the floral homeotic genes, the class C gene *AGAMOUS* (*AG*) is involved in carpel and stamen specification in *Arabidopsis*: *AG* alone promotes carpel development, whereas *AG* together with two class B genes, *APETALA3* (*AP3*) and *PISTILLATA* (*PI*), promotes stamen development (Bowman et al., 1991; Yanofsky et al., 1990; reviewed in Coen and Meyerowitz, 1991). Loss of function of *AG* results in the formation of a set of flower organs consisting of sepal–petal–petal (*ag* flower). The

ectopic formation of petals in whorl 3 is promoted by a combination of class A and class B genes: the former gene is misexpressed in this whorl because of the absence of *AG*, which represses class A gene expression in wild type. Repeated formation of the *ag* flower is caused by loss of determinacy of the flower meristem (Lenhard et al., 2001; Lohmann et al., 2001). In wild type, *AG* induces *KNUCKLES* (*KNU*), which mediates repression of *WUSCHEL* (*WUS*), a stem-cell-promoting gene (Sun et al., 2014; Sun et al., 2009). Via the indirect repression of *WUS* by *AG*, the flower meristem terminates after development of the carpel in wild type (determinate meristem). Thus, *AG* has four functions in the ABC model, namely, carpel specification, stamen specification, promotion of flower meristem determinacy, and repression of class A genes. After carpel formation, *AG* induces two *SHATTER PROOF* (*SHP*) genes, which regulate ovule differentiation (Flanagan et al., 1996; Pinyopich et al., 2003; Savidge et al., 1995). In addition, *CRABS CLAW* (*CRC*) and *SPATULA* are required for the elaboration of carpel morphology together with *AG* (Alvarez and Smyth, 1999; Bowman and Smyth, 1999). *CRC* is also involved in flower meristem determinacy: for example, the *crc knu* double mutant shows an indeterminate flower phenotype (Yamaguchi et al., 2017).

AG encodes a MADS-domain transcription factor, similar to other floral homeotic genes except for *APETALA2* (*AP2*) in *Arabidopsis* (Yanofsky et al., 1990). Phylogenetic studies indicated that MADS genes constitute a large gene family, which is classified into several subfamilies such as class B and class C (reviewed in Becker and Theissen, 2003; Ciaffi et al., 2011; Dreni and Kater, 2014). The *Arabidopsis*

genome has three genes closely related to *AG*: i.e., *SHP1*, *SHP2*, and *STICKSEED* (*STK*). These four genes including *AG* are classified into two classes: class C including *AG* and *SHP*s, and class D including *STK*. Hereafter, we used the term 'class C' (also 'class A' and 'class B') from the viewpoint of gene phylogeny in this paper, but not from the functional aspect based on the ABC model.

Although the ABC model is essentially conserved in angiosperms, the function of individual ABC genes is not necessarily the same among different species, and some modifications seem to be needed for application of the ABC model depending on the plant species. For example, whereas the *AP2* gene in *Arabidopsis* is required to specify sepals and petals and to repress *AG*, the *AP2* ortholog in petunia (*Petunia hybrida*) and *Antirrhinum* does not have this function (Keck et al., 2003; Maes et al., 2001). Instead, microRNAs of the *miR169* family, encoded in the *BLIND* and *FISTULATA* loci in petunia and *Antirrhinum*, respectively, are responsible for restricting expression of the *AG*-like class C genes to the inner whorls (Cartolano et al., 2007). In addition, the function of *Antirrhinum PLENA* (*PLE*) in flower development is similar to that of *Arabidopsis AG*; however, *PLE* is phylogenetically more similar to *SHP*s than to *AG* (Davies et al., 1999).

Species in the grass family (*Poaceae*), such as rice (*Oryza sativa*) and maize (*Zea mays*), generate flowers that are distinct from those of eudicots (reviewed in Hirano et al., 2014; Tanaka et al., 2014; Yoshida and Nagato, 2011). Floral organs are formed within specialized inflorescence units, comprising a spikelet and a floret. In rice, a mature carpel (pistil) formed from three carpel primordia develops in the center of the

spikelet (whorl 4), and six stamens are differentiated around the pistil (whorl 3). Rice flowers lack obvious petals; instead, two semi-transparent small organs, called lodicules (i.e., petal homologs), are formed in whorl 2. These floral organs constitute the floret, together with a palea and a lemma, which enclose the floral organs.

The functions of class B genes that specify the stamens and the petal in *Arabidopsis* are conserved in rice (reviewed in Hirano et al., 2014; Tanaka et al., 2014; Yoshida and Nagato, 2011). In rice, for example, loss of function of *SUPERWOMAN1* (*SPW1*), the *Arabidopsis AP3* ortholog, leads homeotic transformation of stamens and lodicules into carpels and palea-like organs, respectively, similar to the transformation of stamens and petals into carpels and sepals in *Arabidopsis* (Nagasawa et al., 2003). By contrast, the specification of carpel identity is regulated by the *YABBY* gene *DROOPING LEAF* (*DL*), an ortholog of *Arabidopsis CRC*, in rice (Nagasawa et al., 2003; Yamaguchi et al., 2004). Plants with loss of function of *DL* fail to develop carpels, but instead differentiate several stamens in whorl 4. Initiation of carpel development and *DL* expression are coincident in rice (Yamaguchi et al., 2004).

The function of class C genes is somewhat more complex, owing to gene duplication during grass evolution. For example, rice has two class C genes, *OsMADS3* and *OsMADS58*, in the *AG* subfamily (Yamaguchi et al., 2006). Yamaguchi et al. (2006) in my laboratory previously reported that they regulate stamen specification and flower meristem determinacy, and the functions of the two genes have partially diversified. Because carpel-like organs develop in an *osmads3* mutant in which *OsMADS58* expression is silenced, Yamaguchi et al. speculated that the contribution of class C

genes to carpel specification is weak. However, another group reported that the class C genes in rice promote carpel specification but *DL* does not (Dreni et al., 2011). Thus, the gene responsible for carpel specification and the actual role of class C genes remain controversial.

In this study, I have re-addressed the function of class C genes in rice flower development. Yamaguchi et al. (2006) used RNA silencing lines to examine *OsMADS58* function, whereas Dreni et al., (2011) investigated a mutant with an ambiguous mutation (i.e., a transposon insertion in an intron). To obtain more conclusive evidence, therefore, I first observed complete loss-of-function mutants of *OsMADS58* isolated by two methods, TILLING and CRISPR/Cas9. Using null mutants of both *OsMADS3* and *OsMADS58,* I then addressed whether carpels are formed in the absence of the two class C genes. I also investigated which organs are formed by class C genes alone. My phenotypic analysis clearly showed that carpel-like organs differentiated in the absence of the two class C genes, whereas no carpels developed in the presence of these genes in the *dl spw1* double mutant. Thus, the function of class C genes seems to differ between rice and *Arabidopsis*. Lastly, I revealed that *DL* has a crucial function in flower meristem determinacy.

Results

Flower phenotypes of class C mutants

The original *osmads58* mutant (a kind gift from Dr. M. Kater) has an insertion of *dSpm* element in the second intron of *OsMADS58* (Dreni et al., 2011). Preliminary experiment performed in my laboratory indicated that this mutant, which showed wild type-like flower phenotype, produced normal transcripts in which the large second intron containing the transposon was removed. This unexpected expression might have occurred due to an unstable mutation by transposon insertion.

Thus, I tried to analyze the phenotypes of complete loss-of-function mutants of *OsMADS58*. First, I disrupted the *OsMADS58* gene by the CRISPR/Cas9 method (Mikami et al., 2015) and obtained a biallelic mutant, named *osmads58-cas9*, in which a one-base insertion in exon 3 caused a frame-shift mutation (Fig. 2-1). Second, I used an allele, *osmads58-7*, with a mutation at the 5' splice site of the first intron, which had been isolated by Dr. Y. Yasui using the TILLING method (Suzuki et al., 2008; Satoh et al., 2010). Although *OsMADS58* function was completely lost in both *osmads58-cas9* and *osmads58-7* mutants, no obvious abnormality was observed in the flowers of either plant (Fig. 2-2 A-C).

Next, I observed the flowers of another class C mutant, *osmads3-fe1* (Yasui et al., 2017). As described previously (Yasui et al., 2017), a chimeric organ consisting of lodicules and stamens was produced, in place of stamens, in expanded whorl 3 (Fig. 2-2 D). This phenotype indicated that *OsMADS3* is partially involved in stamen

specification.

I then analyzed flower phenotypes of the *osmads3-fe1 osmads58-7* double mutant. *osmads3-fe1 osmads58-7* flowers showed a marked phenotype in which stamens failed to form, and lodicules and green carpel-like organs were repeatedly formed (Fig. 2-2 E). The complete loss of stamens in *osmads3-fe1 osmads58-7* indicated that both *OsMADS3* and *OsMADS58* are required for specifying stamen identity. Furthermore, the repeated formation of lodicules and green carpel-like organs suggested that both *OsMADS3* and *OsMADS58* play a critical role in flower meristem determinacy (see below). Based on the phenotype of the two single mutants, the contribution of *OsMADS3* to the specification of stamen identity seems to be greater than that of *OsMADS58*.

Identity of carpel-like organs in *osmads3-fe1 osmads58-7*

To characterize the identity of the green carpel-like organ in *osmads3-fe1 osmads58-7*, I used scanning electron microscopy (SEM) to compare the epidermal morphology of this organ with that of flower organs in wild type (Fig. 2-3 A-B). The carpel, anther, and palea in wild type showed features characteristic of their epidermal morphology (Fig. 2-3 C-E). Among these organs, the epidermis of the green organ in *osmads3-fe1 osmads58-7* was most similar to that of the carpel in wild type: the cells were flat rectangles and arranged in parallel to make cell files (Fig. 2-3 B). This result strongly suggested that the green organ in *osmads3-fe1 osmads58-7* had carpel identity. However, additional features, such as a hair-like structure and other epidermal

morphology, were also present in the green carpel-like organ (Fig. 2-3 A) (see below).

To verify that the green carpel-like organ had carpel identity, I examined the spatial expression pattern of *DL*, which regulates carpel specification and is expressed in the carpel primordia throughout its development (Yamaguchi et al., 2004). First, I confirmed that *DL* is expressed in the carpel primordia in wild-type flowers (Fig. 2-3 F). *DL* signal was also observed in the lemma; however, this signal corresponds to the localized expression of *DL* in the lemma midrib, similar to its expression in the leaf midrib (Fig. 2-3 G) (Ohmori et al., 2011; Yamaguchi et al., 2004). In *osmads3-fe1 osmads58-7*, *DL* was expressed in the primordia of the green carpel-like organ from its initiation and was uniformly expressed in this organ during its development (Fig. 2-3 J, L). I then examined the expression of *OsMADS13*, which is involved in ovule development in rice (Dreni et al., 2011; Yamaki et al., 2011). Expression of *OsMADS13* was observed in the presumptive ovule primordia and adaxial region of the carpel primordia in wild type (Fig. 2-3 I). In *osmads3-fe1 osmads58-7*, *OsMADS13* expression was observed on the adaxial side of the carpel-like organ (Fig. 2-3 N). Taken altogether, these results indicated that the green carpel-like organ of *osmads3-fe1 osmads58-7* has the characteristics of wild-type carpel identity.

Despite this conclusion, the carpel-like organ showed morphological features additional to those of the wild-type carpel, as described above. To determine the origin of these additional features, I examined the expression of *OsMADS15*, which is responsible for lemma/palea identity (Wu et al., 2017). Expression of *OsMADS15* was observed in the developing lemma in wild type (Fig. 2-3 H). In *osmads3-fe1 osmads58-*

7, weak *OsMADS15* expression was detected in the early primordia of the carpel-like organ, in addition to the lemma (Fig. 2-3 K). *OsMADS15* expression was also observed on the abaxial side of this organ at a subsequent developmental stage (Fig. 2-3 M; note that Fig. 2-3 J and 2-3 K, and Fig. 2-3 L and 2-3 M, are consecutive sections). Thus, *DL* and *OsMADS15* seem to be simultaneously expressed in the green carpel-like organ in *osmads3-fe1 osmads58-7*. Thus, weak expression of *OsMADS15* seems to partially affect the epidermal morphology of the carpel-like organ.

Expression of *SPW1*, a class B gene, was observed in the lodicules and stamens in wild type (Fig. 2-3 O). This gene was strongly expressed in the lodicules, which repeatedly formed in *osmads3-fe1 osmads58-7* (Fig. 2-3 P), confirming that it is responsible for lodicule development. By contrast, *SPW1* expression was downregulated in the carpel-like organ (Fig. 2-3 P), where strong expression of *DL* was detected (Fig. 2-3 Q).

In summary, given the multiple lines of evidence indicating that the green organs in the *osmads3-fe1 osmads58-7* double mutant have carpel identity, it seems unlikely that the activity of class C genes is required for carpel specification in rice.

Loss of flower meristem determinacy in *osmads3-fe1 osmads58-7*

To examine the meristem indeterminacy of *osmads3-fe1 osmads58-7* in detail, I examined mature flowers just before heading by SEM. At this growth stage, the carpels had already developed and the flower meristem had disappeared in wild type (Fig. 2-2 A). In *osmads3-fe1 osmads58-7*, by contrast, the flower meristem was detected at the

apical region of the mature flower (Fig. 2-4 A). Repeated differentiation of lodicules from the flower meristem was also observed.

Next, I examined the expression pattern of the class I *KNOX* gene *OSH1*, which is a marker of meristematic indeterminate cells (Sato et al., 1996; Yamaguchi et al., 2004). Although *OSH1* was expressed in the flower meristem at an early developmental stage in wild type (Fig. 2-4 B), *OSH1* expression was not observed after carpel development, suggesting that the flower meristem had disappeared (Fig. 2-4 C). In *osmads3-fe1 osmads58-7*, by contrast, *OSH1* expression was clearly observed even at the growth stage when carpels had initiated in wild type (Fig. 2-4 D). This observation suggests that the flower meristem remains active in *osmads3-fe1 osmads58-7* at a late stage of flower development. Accordingly, *OsMADS3* and *OsMADS58* are likely to play an important role in regulating the determinacy of the flower meristem.

fon2 **mutation enhances the indeterminate nature of the flower meristem in** ***osmads3 osmads58***

Next, I analyzed the genetic interaction of class C genes with the *FLORAL ORGAN NUMBER2* (*FON2*) gene, an ortholog of *Arabidopsis CLAVATA3* (*CLV3*) (Fletcher et al. 1999; Suzaki et al. 2006). *FON2* negatively regulate stem cell proliferation, similar to *CLV3*, and loss of its function results in enlargement of the flower meristem (Suzaki et al. 2006). I analyzed flower phenotypes of double and triple mutants consisting of *osmads3-fe1*, *osmads58-7*, and *fon2-3*.

As reported previously (Suzaki et al. 2006), *fon2-3* showed an increase in

floral organ number, especially carpels (Fig. 2-5 A). The flower of *osmads58-7 fon2-3* resembled the *fon2-3* flower (Fig. 2-5 B), consistent with my above observation that the *osmads58* single mutant showed no abnormality. By contrast, *osmads3-fe1 fon2-3* showed a marked flower phenotype, namely, the formation of multiple carpels (Fig. 2-5 C), consistent with the previous observation (Yasui et al. 2017).

Next, I observed plants heterozygous for *osmads3-fe1* and homozygous for both *osmads58-7* and *fon2-3* (designated *osmads3-fe1*/+ *osmads58-7 fon2-3*) (Fig. 2-5 D). The flower phenotype of these plants was milder than that of *osmads3-fe1 fon2-3* (Fig. 2-5 C). This result indicated that one wild-type allele of *OsMADS3* might be enough to specify stamen identity, and might have stronger function than two wild-type alleles of *OsMADS58*. In the *osmads3-fe1 osmads58-7*/+ *fon2-3* flower, by contrast, no normal stamens were formed, although an undeveloped anther-like tissue was detected in a chimeric organ (Fig. 2-5 E). This result also indicated that *OsMADS58* has weak function for stamen specification.

The *osmads3-fe1 osmads58-7 fon2-3* triple mutant showed severe defects in the flower (Fig. 2-5 F, G). The mature flower just before heading resembled that of *osmads3-fe1 osmads58-7*: the lodicule and carpel-like organs were repeatedly formed (Fig. 2-2 E, Fig. 2-5 F). Unlike *osmads3-fe1 osmads58-7*, however, flower development persisted in the *osmads3-fe1 osmads58-7 fon2-3* triple mutant after heading, resulting in the formation of branched clusters of lodicules and carpel-like organs (Fig. 2-5 G). Furthermore, the formation of large numbers of these organs persisted even at 1 month after heading. I detected a meristem-like dome structure on the top of each of the floral

branch by SEM analysis (Fig. 2-5 I). In situ hybridization showed clear *OSH1* signals in the meristem-like domes (Fig. 2-5 J, K). These results indicated that meristem indeterminacy is strongly promoted in the *osmads3-fe1 osmads58-7 fon2-3* triple mutant. Probably due to the high accumulation of stem cells and enlargement of the meristem, the flower meristem in the *osmads3-fe1 osmads58-7 fon2-3* triple mutant seemed to be divided into several sub-meristems, which continued to produce branched clusters of lodicules and carpel-like organs over a long period. Thus, *fon2* mutation enhanced the indeterminate nature of the flower meristem in *osmads3-fe1 osmads58-7.*

SEM observation confirmed that the carpel-like organ in *osmads3-fe1 osmads58-7 fon2-3* had an epidermis highly similar to that of the wild-type carpel, even in the region where the ectopic hair-like structure was produced (Fig. 2-5 L). Lastly, green organs, which were more similar to wild-type carpels owing to a lack of hairs, were observed at the apical region of the floral organ clusters (Fig. 2-5 H).

Unidentifiable organs form in the *dl spw1* mutant

In *Arabidopsis*, the class C gene *AG* alone specifies carpel identity (Bowman et al., 1991; Yanofsky et al., 1990). However, my above findings indicated that class C genes seems to be not involved in carpel specification in rice. This led me to question which floral organ is specified by class C genes when they function alone without other floral homeotic genes. According to modified ABC model of rice flower development (reviewed in Hirano et al., 2014; Tanaka et al., 2014), the removal of *DL* and *SPW1* activities should enable me to examine the function of class C genes alone because only

two class C genes would be expressed in whorl 3 and whorl 4.

I therefore analyzed a double mutant of *dl* and *spw1*. Multiple stamens were produced in place of the carpel in whorl 4 in the *dl-sup1* single mutant (Fig. 2-6 A), whereas an indefinite number of carpels were formed instead of stamens in whorl 3 in the *spw1* mutant (Fig. 2-6 B), as described previously (Nagasawa et al., 2003; Yamaguchi et al., 2004). By contrast, the *dl-sup1 spw1-11* double mutant showed a marked phenotype: no flower organs similar to those in wild type were formed. In whorl 2, lodicules were replaced by palea-like organs, which also resembled leaves (Fig. 2-6 C). In the inner whorls, probably corresponding to whorl 3 and whorl 4, unknown white organ clusters were produced (Fig. 2-6 D). Analysis of the inner tissues in cross and longitudinal sections and a magnified SEM image showed that these white organs did not resemble any wild-type floral organ, including carpels, stamens, and lodicules (Fig. 2-6 E-G). The epidermal surface of these unidentifiable organs was different from that of known flower organs including the carpel (Fig. 2-3 C-E and Fig. 2-6 H). Thus, the inner whorls of the *dl-sup1 spw1-11* flower were filled with clusters of unidentifiable organs.

I then examined the expression of the class C gene *OsMADS3*. This gene was expressed in the stamen and carpel primordia in wild type (Fig. 2-6 I). In *dl-sup1 spw1-11*, *OsMADS3* was detected in the apical region of the clusters of unidentifiable organs, confirming that class C genes alone cannot specify any type of flower organ including the carpel (Fig. 2-6 J, K). *OsMADS13* expression was detected (Fig. 2-7), probably due to the induction of *OsMADS13* by class C genes despite the failure in carpel

development in *dl-sup1 spw1-11*.

Flower meristem determinacy is highly compromised in the *dl spw1* mutant

As described above, several unidentifiable organs were produced in the *dl-sup1 spw1-11* flower (Fig. 2-6 D, E). SEM observation revealed a vast number of small planar or tube-like structures, hereafter called "phylloid organs", in the apical region of the unidentifiable organs (Fig. 2-8 A, B). I also observed a meristem-like dome structure, which was surrounded by these "phylloid organs" (Fig. 2-8 B). In addition, many of these meristem-like structures were present in the *dl-sup1 spw1-11* flower (Fig. 2-8 A). Longitudinal sections of the flower further indicated that the basal parts ("stalks") of the unidentifiable organs were branched (Fig. 2-6 F), and produced many "phylloid" organs in the apical region (Fig. 2-8 A, B).

In situ analysis showed that *OSH1* was expressed strongly at the top of the cluster of unidentifiable organs, probably corresponding to the meristem-like dome, in the *dl-sup1 spw1-11* flower (Fig. 2-8 C). In some cases, the meristem-like tissues were close to each other (Fig. 2-8 D). Strong *OSH1* expression was also detected in the stalks (Fig. 2-8 C, D). These results indicated that the dome-like structure contains meristematic indeterminate cells. Therefore, it is likely that the *dl-sup1 spw1-11* flower has the ability to generate "phylloid organs" from these meristematic tissues, even at a mature developmental stage when the wild-type flower has completed flower organ development. Thus, the "phylloid organs" seem to be repeatedly formed in *dl-sup1 spw1-1*. My in situ hybridization results showed that *OsMADS3* was expressed in the

apical region of the unidentifiable organs (Fig. 2-6 J, K). This *OsMADS3*-expressing region might correspond to young "phylloid organs" differentiating from the meristem.

The strong loss of determinacy of the flower meristem in the *dl-sup1 spw1-11* double mutant was unexpected. I therefore examined the expression of *OSH1* in single *dl-sup1* and *spw1-11* mutants. Expression of *OSH1* persisted after stamen formation in whorl 4 in the *dl-sup1* flower (Fig. 2-8 E), consistent with the formation of multiple stamens in whorl 4 (Fig. 2-6 A). In *spw1*, *OSH1* expression was also detected in the apical part of the flower after the differentiation of multiple carpels (Fig. 2-8 F). In the *dl-sup1 spw1-11* double mutant, therefore, the partial loss of meristem determinacy of the *dl* flower seems to be enhanced by combination with the *spw1* mutant, in which meristematic tissues remained in the maturing flower.

Discussion

In this study, I revealed that the carpel-like organs were formed in the absence of class C genes by examining a complete loss-of-function mutant of *OsMADS3* and *OsMADS58*. Conversely, I also showed that no carpel-like organs were differentiated in the presence of class C genes alone by examining a *dl spw1* mutant in which class C genes only were expressed in whorl 3 and whorl 4. Taking these observations together, I concluded that class C genes are not a key regulator for carpel specification in rice. Furthermore, I demonstrated that class C genes and *DL* have a crucial function in the regulation of flower meristem determinacy. Fig. 2-9 summarizes the current model of rice flower development and the roles of the floral homeotic genes.

Class C genes are not a key regulator for specifying carpel identity in rice

To elucidate the function of class C genes, I observed complete loss-of-function mutants of *OsMADS58*, namely, *osmads58-cas9* and *osmads58-7*, isolated via two independent methods, CRISPR/Cas9 and TILLING. Neither mutant showed an obvious abnormality in the flowers, consistent with the results previously reported by Dreni et al. (Dreni et al., 2011). Because a combination of *osmads58* with *osmads3* led serious defects in flower development, it seems likely that loss of *OsMADS58* is compensated by *OsMADS3* activity.

Two opposing views on the gene responsible for carpel specification have been proposed: in one, carpel identity is specified by *DL* (Yamaguchi et al., 2004); in

the other, it is specified by two class C genes, *OsMADS3* and *OsMADS58* (Dreni et al., 2011). To examine the latter possibility, I analyzed a double mutant of class C genes using two complete loss-of-function alleles, *osmads3-fe1* and *osmads58-7* (Yasui et al., 2017 and this study). The *osmads3-fe1 osmads58-7* flower produced repeated lodicules and green carpel-like organs. I examined the identity of the green carpel-like organ by focusing on three characteristics: epidermal morphology, and the expression pattern of *DL* and *OsMADS13*. All data supported the idea that the green carpel-like organ indeed has carpel characteristics.

Despite of these lines of evidence, the carpel-like organ had a few characteristics other than those of a carpel, including the production of hair-like structures and partial disruption of the carpel-like epidermal surface. These additional characteristics seem to be partly caused by the misexpression of *OsMADS15*, which is known to be expressed in the lemma and palea and is needed for their identities (Kyozuka et al., 2000; Wu et al., 2017). *OsMADS15* misexpression is likely to be due to the lack of repression of the class A gene *OsMADS15* by class C genes in *osmads3 osmads58*. Li et al., (2011) reported that, in whorl 4 of the *dl osmads3* double mutant, lodicule-like organs are repeatedly formed but no carpel-like organs are formed (Li et al., 2011). That study supports my idea that differentiation of the green organ is promoted by *DL* in *osmads3 osmads58*. Taken together, the observations suggest that the green organs with carpel identity were formed in the absence of both *OsMADS3* and *OsMADS58*, suggesting that these class C genes are not required for carpel specification (Fig. 2-9).

The involvement of class C genes in carpel specification was also refuted by my analysis of the *dl spw1* double mutant. Among the floral homeotic genes in this double mutant, only class C genes should be expressed in whorl 3 and whorl 4 (Fig. 2-9). My analysis showed that no carpels were formed in this region, despite the clear expression of *OsMADS3*. Thus, the carpel is not specified in the presence of class C genes alone. However, I do not exclude the possibility that *OsMADS3* cannot induce genes necessary for carpel specification, which act together with *DL*.

In *Arabidopsis*, the carpels are specified by the class C gene *AG* alone (Fig. 2-9 B) (Bowman et al., 1991; Yanofsky et al., 1990; reviewed in Coen and Meyerowitz, 1991), and overexpression of *AG* transforms the sepal into carpel-like organs (Mizukami and Ma, 1992). Thus, *AG* is a key regulator in *Arabidopsis*, which is necessary and sufficient for carpel specification. By contrast, no carpel-like organs are generated by the overexpression of *OsMADS3* (*RAG*) (Kyozuka and Shimamoto, 2002), although lodicules are transformed into stamens, similar to the transformation of petals into stamens in *Arabidopsis* overexpressing *AG*.

Taking the evidence altogether, I conclude that class C genes are not a key regulator for carpel specification in rice (Fig. 2-9 B).

Similar flower phenotypes of *osmads3 osmads58*, namely, the repeated formation of lodicules and green organs, were also reported by Dreni et al., (Dreni et al., 2011). However, those authors concluded that carpel specification is regulated by class C genes. Their disagreement with my conclusion is likely to result from insufficient analysis and misleading interpretation of the green organs. Despite their observation of

DL and *OsMADS13* expression within these organs, Dreni et al. considered them to be palea-like, not carpel-like. In particular, their conclusion seems to dismiss the importance of *DL* function (see below). Although I agree that the green organ has partial lemma/palea-like identity, I believe that this identity is conferred by misexpression of the class A gene *OsMADS15* due to the loss of class C activities. Therefore, a more logical idea is that the green organ in *osmads3 osmads58* has mainly carpel identity, and the lemma/palea-like character is partially superimposed on this carpel identity. Consistent with this idea, no green organs were observed in lodicule clusters in whorl 4 of an *osmads3 dl* double mutant, as described above (Li et al., 2011). My idea could be tested by generating an *osmads3 osmads58 dl* triple mutant and observing whether the green carpel-like organs disappear.

Specification and morphogenesis of the carpel

The carpel is specified by the *YABBY* gene *DL* in rice (Yamaguchi et al., 2004). Mutants with loss of function of *DL* fail to initiate carpels and form stamens at the expense of carpels. *DL* is expressed both in the presumptive region of carpel primordia in the flower meristem and in developing carpels in wild type. In the *spw1* mutant, in which stamens are transformed into carpels, *DL* expression is detected in both the original and ectopic carpel primordia, indicating a strong correlation between carpel initiation and *DL* expression (Yamaguchi et al., 2004). The *dl* mutation in combination with other floral homeotic mutants, such as *dl spw1* and *dl osmads3*, is associated with a failure of carpel specification (in this study and (Li et al., 2011; Nagasawa et al., 2003)).

Collectively, these observations support the idea that *DL* plays a critical role in carpel identity in rice. To confirm this conclusion, it is necessary to show that *DL* is sufficient to promote carpel identity. For this purpose, we have to overcome the problem that the simple overexpression of *DL* results in growth arrest at a seedling stage due to leaf thickening (Yamaguchi et al., 2004).

In rice, the pistil (mature carpel) constitutes a bottle-shaped ovary and stigmatic tissues on a style. Although a carpel-like structure was formed in the *osmads3-fe1 osmads58-7* mutant, it differed from the morphology of a complete pistil; for example, it lacked stigmatic tissues and had an unfused ovary wall. By contrast, the combination of at least one wild-type allele of *OsMADS3* or *OsMADS58* together with *DL* resulted in normal-looking pistils in the *osmads3-fe1*/+ *osmads58-7 fon2-3* and *osmads3-fe1 osmads58-7*/+ *fon2-3* plants. Therefore, class C genes seemed to be required to elaborate the morphology of a mature pistil. In addition, because ovules did not differentiate despite the presence of *OsMADS13* expression in *osmads3-fe1 osmads58-7*, class C activity is also likely to be required for ovule differentiation. *DL* is expressed in *osmads3 osmads58* (this study; Dreni et al., 2011), and both *OsMADS3* and *OsMADS58* are expressed in *dl* (Yamaguchi et al., 2006). It therefore seems likely that class C genes do not regulate the expression of *DL*, and vice versa.

Regulation of flower meristem determinacy

Flower meristem determinacy was strongly compromised in *osmads3 osmads58* (Fig. 2-4), consistent with several previous reports (Dreni et al., 2011; Yamaguchi et al., 2006).

In addition to the repeated formation of lodicules and carpel-like organs, the flower meristem, which expressed *OSH1*, remained even in the mature flowers of *osmads3 osmads58*. This flower meristem indeterminacy was highly enhanced in the *osmads3 osmads58 fon2* triple mutant: for example, clusters consisting of a number of lodicules and carpel-like organs were branched, probably due to splitting of an enlarged flower meristem. Thus, this enhanced indeterminacy seems to be associated with an excess accumulation of stem cells caused by *fon2* mutation.

Flower meristem determinacy was also strongly reduced in the *dl spw1* double mutant. A large number of unidentifiable organs were formed repeatedly and several flower meristems remained in clusters of these organs. The formation of an indefinite number of ectopic stamens in whorl 4, coupled with prolonged expression of *OSH1*, in the *dl* single mutant suggested that *DL* is partially involved in meristem determinacy, as reported previously (Yamaguchi et al., 2004). However, the enhancement of this partial indeterminacy in *dl* by *spw1* mutation was unexpected, because class B gene involvement in flower determinacy has not previously been described in rice or other plants.

Unlike in *Arabidopsis*, the flower meristem remains between the carpel primordia to differentiate an ovule in rice (Dreni et al., 2011; Yamaki et al., 2011). Therefore, a *spw1* flower producing many pistils would be expected to maintain several sets of indeterminate tissues after carpel initiation. Indeed, *OSH1* expression was detected in several parts of the *spw1* flower. These indeterminate tissues are also likely to remain in the *dl spw1* mutant, although unidentifiable organs were observed instead

of carpels. It is possible that, in the *dl spw1* mutant, these meristematic tissues are maintained as dome-like meristems that independently and repeatedly differentiate unidentifiable organs. Thus, the enhanced indeterminacy of the *dl spw1* flower seems to be associated with the remaining meristematic tissues within the multiple carpels in the *spw1* mutant. In the *Arabidopsis crc pi* mutant, indeterminate flowers are not formed, probably because the flower meristem is consumed by carpel formation in the *pi* single mutant (Alvarez and Smyth, 1999).

In *Arabidopsis*, *CRC* is also involved in the promotion of flower meristem determinacy (Fig. 2-9). Although a *crc* single mutant produces determinate flowers, meristem determinacy is strongly reduced in *crc ag*/+ and *crc knu* double mutants (Alvarez and Smyth, 1999; Yamaguchi et al., 2017). In petunia (*Petunia hybrida*), loss of the function of two *CRC* orthologs, without combination with other mutations, leads to severe defects in flower determinacy (Morel et al., 2018). Furthermore, *CRC* orthologs are also involved in meristem determinacy in a basal eudicot, *Eschscholzia californica* (Orashakova et al., 2009). Accordingly, involvement of *CRC/DL* in flower meristem determinacy seems to be part of a widely conserved mechanism in angiosperms. By contrast, the role of the *CRC/DL* genes in flower organ formation differ between rice and *Arabidopsis*. Whereas *DL* specifies carpel identity in rice (Nagasawa et al., 2003; Yamaguchi et al., 2004), *CRC* does not have this function and instead contribute to the elaboration of carpel morphology (Alvarez and Smyth, 1999; Bowman and Smyth, 1999). In addition, *CRC* is required for nectary development (Bowman and Smyth, 1999), but *DL* lacks this function and is required for midrib

formation in the leaf (Nagasawa et al., 2003; Ohmori et al., 2011; Yamaguchi et al., 2004). Furthermore, *DL* and class C genes do not regulate each other's expression, as described above, whereas *CRC* is a direct target of *AG* (Gomez-Mena, et al. 2005).

The function of class C genes in rice

Apart from carpel specification, *OsMADS3* and *OsMADS58* redundantly regulated stamen specification, repression of class A genes, and flower meristem determinacy (Fig. 2-9). For each type of regulation, the contribution of *OsMADS3* seems to be slightly stronger than that of *OsMADS58*. Although the paper from my laboratory (Yamaguchi et al., 2006) stated previously that the functions of class C genes have partially diversified, large functional differences between the two genes were not observed in the present study. The disagreement between two studies seems to result from the phenotype of the *OsMADS58 RNA* silencing line, which might have been caused by unexpected simultaneous downregulation of *OsMADS3* and *OsMADS58*.

In *Arabidopsis*, *AG* regulates carpel specification in addition to the three functions described herein for class C genes in rice. In the context of Goethe's idea that flower organs are modified leaves (Goethe, 1790), ABC genes seem to add floral organ identity to the leaf. Indeed, leaf-like organs are formed in the *ap2 pi* (or *ap3*) *ag* triple mutant, whereas *AG* expression alone promotes carpel development in the *ap2 pi* double mutant (Bowman et al., 1991). On the basis of this concept, the development of the unidentifiable organs, which differs from leaves, in *dl spw1* mutants suggests that rice class C genes also add some characteristics to leaves, although they do not specify

carpel identity. In future studies, it will be essential to determine which genes are regulated by *DL*, class C genes, and both *DL* and class C genes, and to elucidate the relationship between the function of those downstream genes and organ identity.

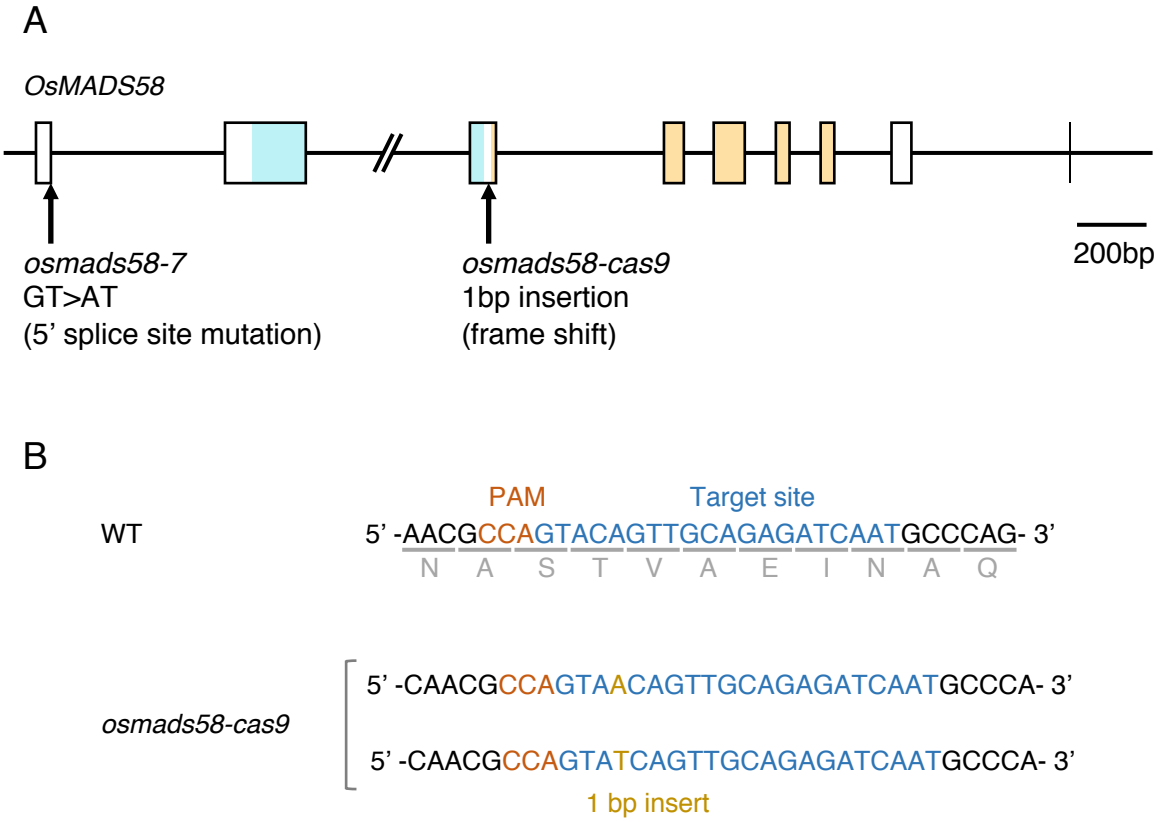

Fig. 2-1 Schematic representation of *OsMADS58*.
(A) The *OsMADS58* gene, showing the position of the mutations in *osmads58-cas9* and *osmads58-7*. Boxes indicate coding regions; solid lines indicate UTRs and introns. Blue box, MADS domain; orange box, K domain.
(B) Sequence of the mutated region in *osmads58-cas9*.

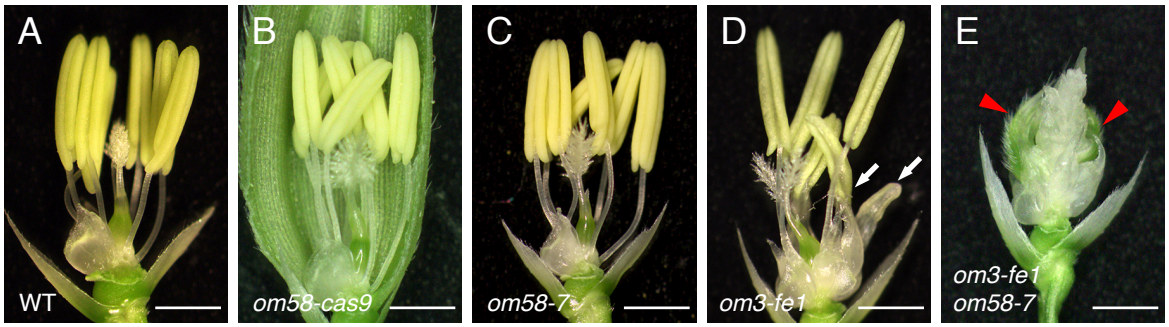

Fig. 2-2 Phenotypes of mature flowers.
(A) Wild type.
(B) *osmads58-cas9*.
(C) *osmads58-7*.
(D) *osmads3-fe1*. Arrow indicates chimeric organs consisting of lodicules and stamens.
(E) *osmads3-fe1 osmads58-7*.
Red arrowheads indicate the green carpel-like organs. The lemma and palea are completely or partially removed. *om, osmads*. Scale bars = 1mm.

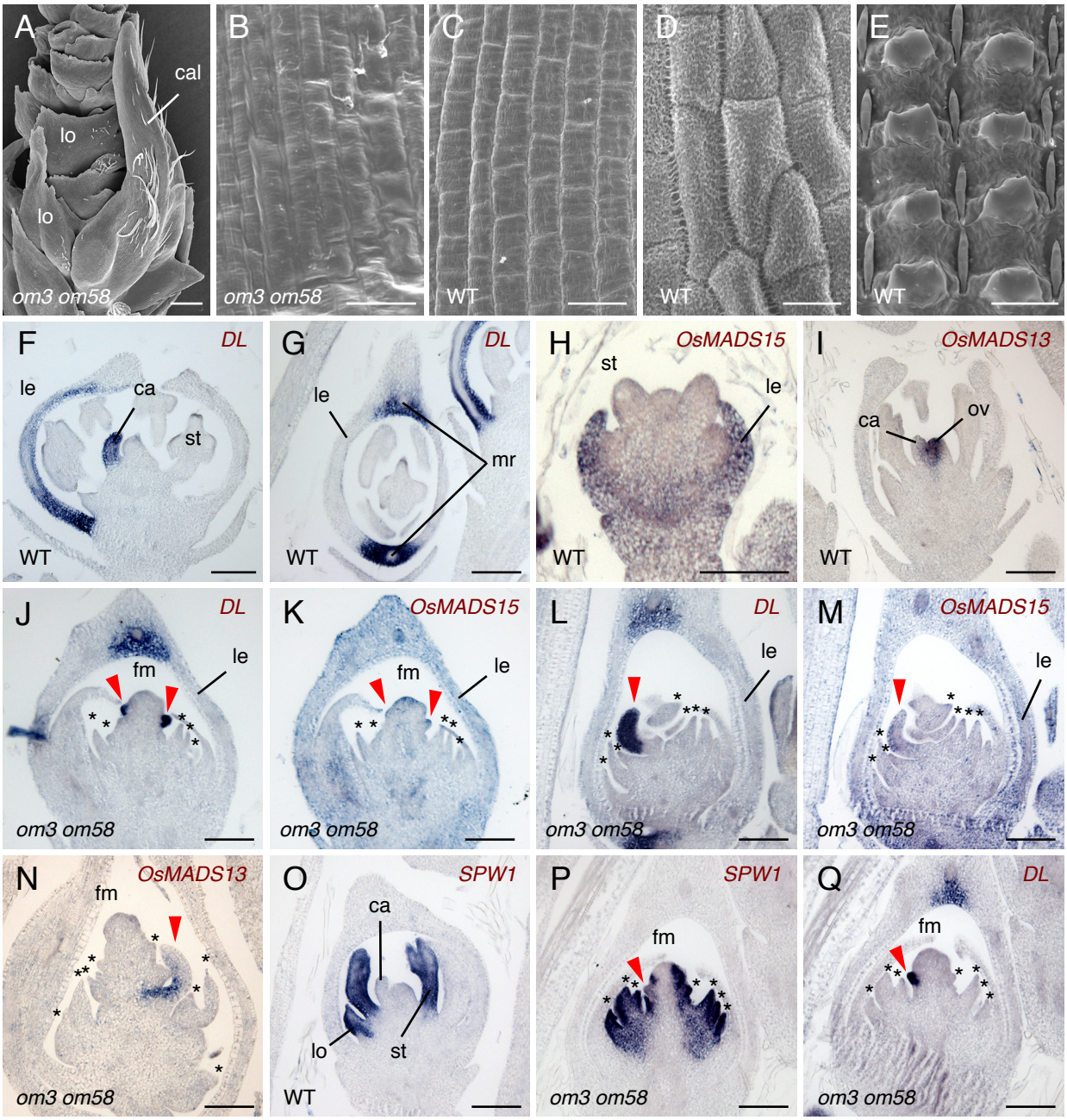
A
cal
lo
lo
om3 om58
B
om3 om58
C
WT
D
WT
E
WT
F
DL
le
ca
st
WT
G
DL
le
mr
WT
H
OsMADS15
st
le
WT
I
OsMADS13
ca
ov
WT
J
DL
fm
le
om3 om58
K
OsMADS15
fm
le
om3 om58
L
DL
le
om3 om58
M
OsMADS15
le
om3 om58
N
OsMADS13
fm
om3 om58
O
SPW1
ca
lo
st
WT
P
SPW1
fm
om3 om58
Q
DL
fm
om3 om58

Fig. 2-3 Identity of the green carpel-like organs in *osmads3-fe1 osmads58-7*.
(A) SEM image of the carpel-like organs and lodicules in *osmads3-fe1 osmads58-7*.
(B) SEM image of the epidermal morphology of a carpel-like organ in *osmads3-fe1 osmads58-7*.
(C-E) SEM images of the epidermal morphology of the carpel (C), anther (D), and palea (E) in wild type.
(F-I, O) In situ hybridization of *DL* (F, G), *OsMADS15* (H), *OsMADS13* (I), and *SPW1* (O) in wild type.
(J-M) In situ hybridization of *DL* (J, L) and *OsMADS15* (K, M) in *osmads3-fe1 osmads58-7*. Strong *DL* expression and weak *OsMADS15* expression are detected in the initiating primordia of the carpel-like organ (J, K). In the developing carpel-like organ, *DL* expression is detected uniformly (L), whereas weak *OsMADS15* expression is detected in the abaxial region (M).
(N, P, Q) In situ hybridization of *OsMADS13* (N), *SPW1* (P), and *DL* (Q) in *osmads3-fe1 osmads58-7*. *OsMADS13* expression is detected in the adaxial region of the developing carpel-like organ (N). *SPW1* expression is downregulated in the carpel-like organ primordium (P), where *DL* is strongly expressed (Q).
Red arrowheads and asterisks indicate the carpel-like organ primordia and lodicules, respectively, in *osmads3-fe1 osmads58-7*. Consecutive sections of the *osmads3-fe1 osmads58-7* flower were used for hybridization in (J and K), (L and M) and (P and Q). ca, carpel; cal, carpel-like organ; fm, flower meristem; le, lemma; lo, lodicule; mr, midrib; *om3*, *osmads3-fe1*; *om58*, *osmads58-7*; ov, ovule; st, stamen. Scale bars = 200 μm (A), 10 μm (B), 20 μm (C, D), 50 μm (E), 100 μm (F-Q).

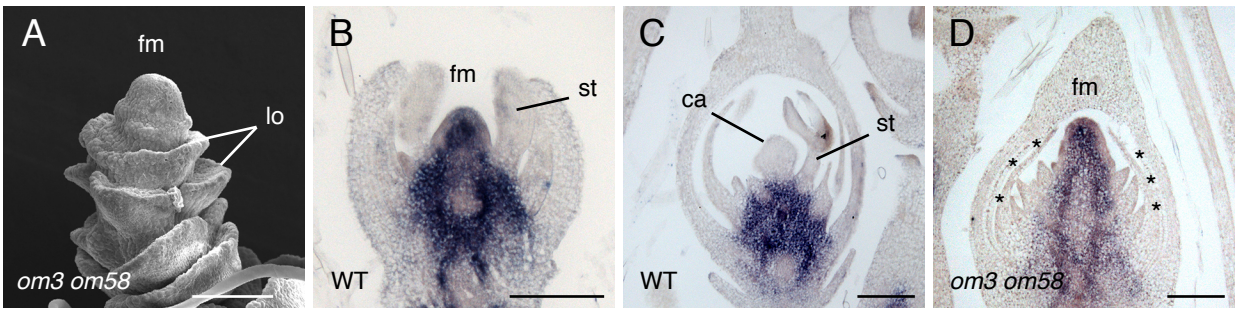

Fig. 2-4 Indeterminacy of the flower meristem in *osmads3-fe1 osmads58-7*.
(A) SEM images of the floral meristem detected at the apical region of the mature flower in *osmads3-fe1 osmads58-7*.
(B, C) In situ hybridization of *OSH1* in wild-type developing flowers just before carpel initiation (B) and after carpel development (C).
(D) In situ hybridization of *OSH1* in *osmads3-fe1 osmads58-7* developing flowers at the same stage as (C).
Asterisks indicate lodicules in *osmads3-fe1 osmads58-7*. ca, carpel; fm, flower meristem; lo, lodicule; *om3*, *osmads3-fe1*; *om58*, *osmads58-7*; st, stamen. Scale bars = 100 μm.

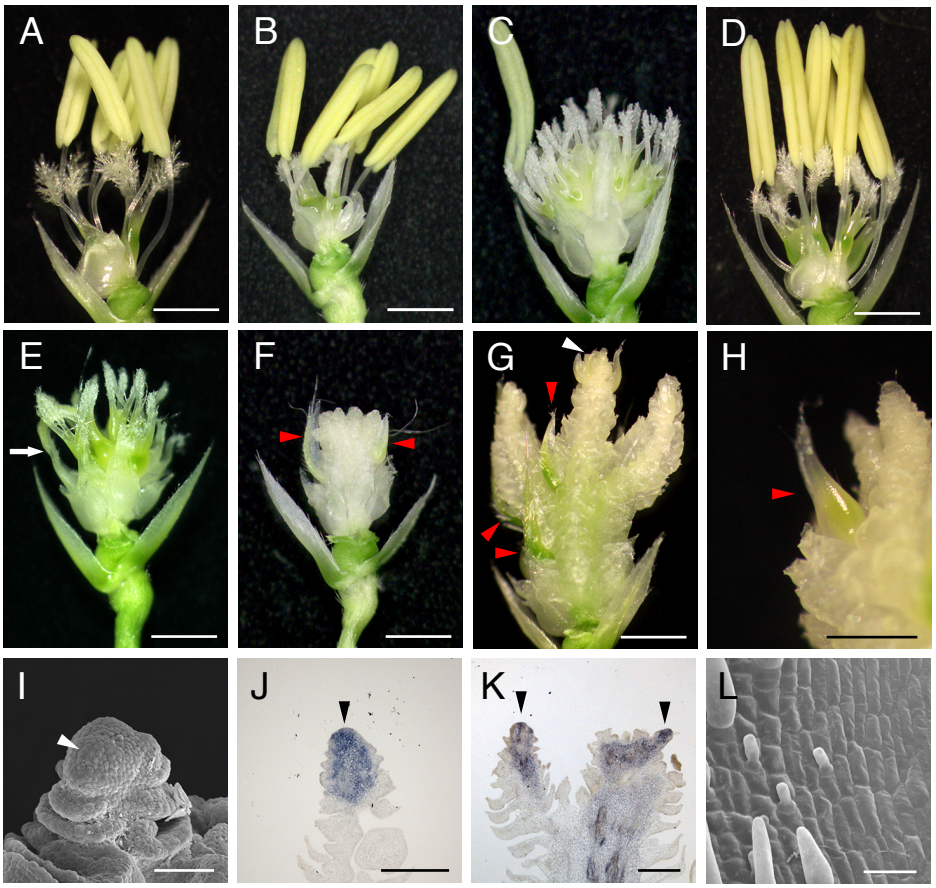

Fig. 2-5 Effect of *fon2* mutation on the *osmads3-fe1 osmads58-7* flower.
(A-G) Phenotypes of the flowers of *fon2-3* (A), *osmads58-7 fon2-3* (B), *osmads3-fe1 fon2-3* (C), *osmads3-fe1*/+ *osmads58-7 fon2-3* (D), *osmads3-fe1 osmads58-7*/+ *fon2-3* (E), and *osmads3-fe1 osmads58-7 fon2-3* (F, G). The *osmads3-fe1 osmads58-7 fon2-3* flower in (G) is one month after heading; all other flowers are just before heading.
(H) Close-up of a carpel-like organ formed in *osmads3-fe1 osmads58-7 fon2-3*.
(I) SEM images of the floral meristem (white arrowhead) detected at the apical region of the mature flower in (G).
(J, K) In situ hybridization of *OSH1* in mature flowers of *osmads3-fe1 osmads58-7 fon2-3*. *OSH1* expression is detected at the top of the flower, corresponding to the flower meristem.
(L) SEM images of the epidermal morphology of a green carpel-like organ in *osmads3-fe1 osmads58-7 fon2-3*.
Red arrowheads indicate the carpel-like organs. White and black arrowheads indicate the flower meristem. White arrow indicates chimeric organs consisting of lodicules and stamens. The lemma and palea are completely removed.
Scale bars = 1 mm (A-G), 500 μm (H), 25 μm (I), 50 μm (J), 200 μm (K, L).

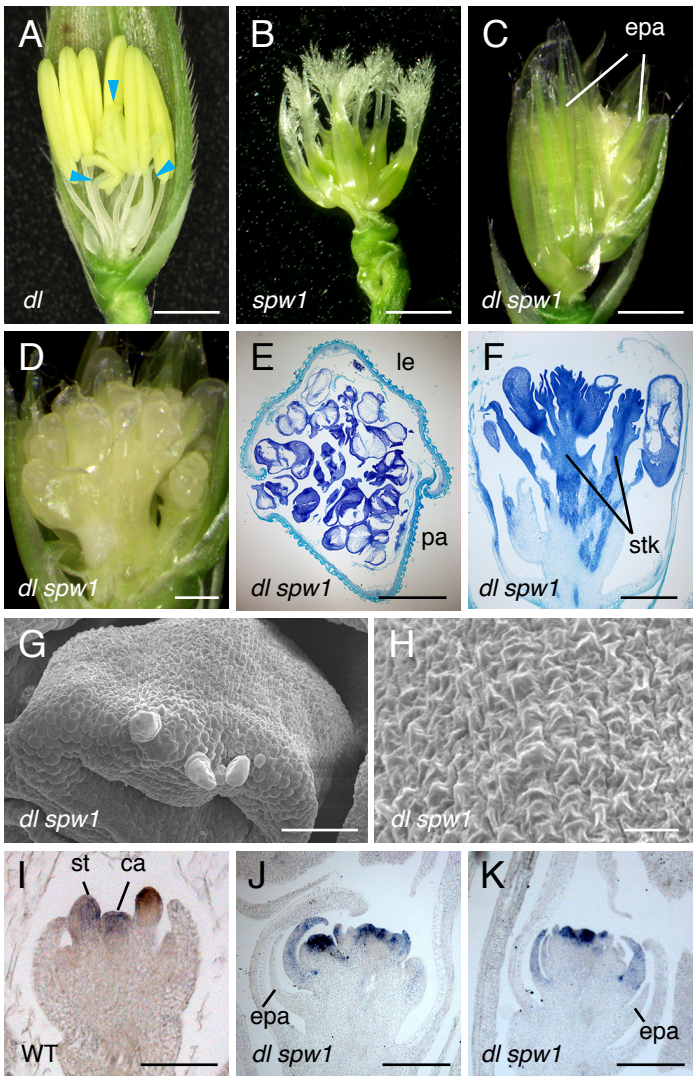

Fig. 2-6 Flower phenotype of the *dl-sup1 spw1-11* double mutant.
(A-D) Flowers just before heading: *dl-sup1* (A), *spw1-11*(B), *dl-sup1 spw1-11* (C, D). Blue arrowhead in (A) indicates ectopic stamens. The ectopic palea-like organs observed in (C) are removed in (D), revealing white unidentifiable organs.
(E, F) Cross (E) and longitudinal (F) sections of the mature *dl-sup1 spw1-11* flower.
(G) Close-up of an unidentifiable organ observed in *dl-sup1 spw1-11* by SEM.
(H) Epidermal morphology of the unidentifiable organ shown in (G).
(I-K) In situ hybridization of *OsMADS3* in the developing flower of wild type (I) and *dl-sup1 spw1-11* (J, K).
ca, carpel; epa, ectopic palea-like organ; le, lemma; pa, palea, st, stamen; stk, stalk. Scale bars = 100 μm (A-D), 500 μm (E, F), 50 μm (G), 10 μm (H), 100 μm (I), 200 μm (J, K).

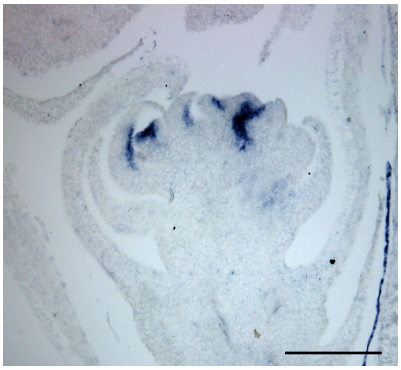

Fig. 2-7 Expression pattern of *OsMADS13* in *dl-sup1 spw1-11*.

Scale bars = 200 μm.

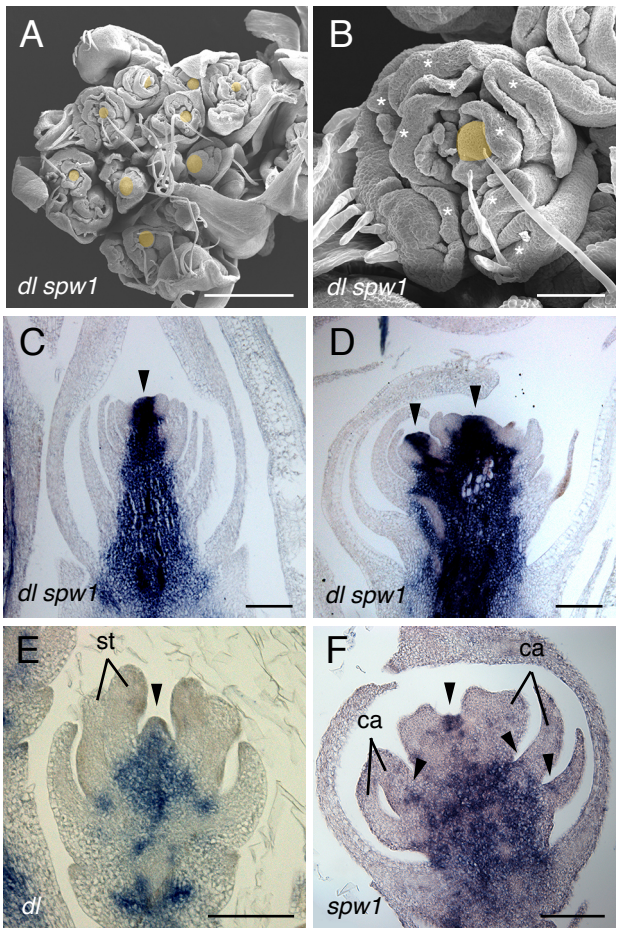

Fig. 2-8 Indeterminacy of the flower meristem in the *dl-sup1 spw1-11* double mutant.
(A) SEM images of the apical region of the unidentifiable organ in *dl-sup1 spw1-11*.
(B) Close-up of a cluster of unidentifiable organs in *dl-sup1 spw1-11*. Meristem-like structures are highlighted in orange; "phylloid organs" are indicated by asterisks.
(C-F) In situ hybridization of *OSH1* in developing flowers of *dl-sup1 spw1-11* (C, D), *dl-sup1* (E), and *spw1-11* (F). The data (F) was provided by Ms. Suzuha Ohmori. *OSH1* expression was detected at the top of the unidentifiable organs and stalks in *dl-sup1 spw1-11* (C, D). *OSH1* expression persisted in *dl-sup1* (E) and *spw1-11* (F).
Arrowheads indicate *OSH1* expression at the meristem-like structure and tissues. ca, carpel; st, stamen. Scale bars = 500 μm (A), 100 μm (B-F).

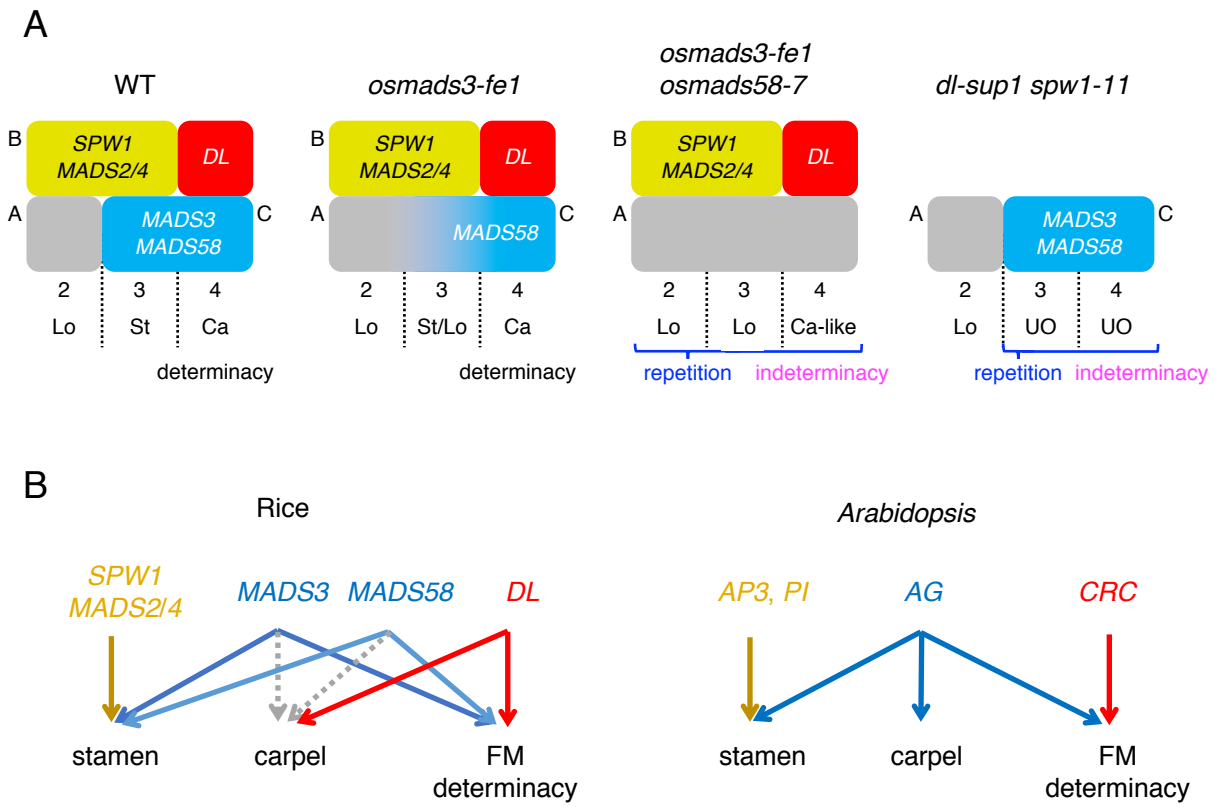

Fig. 2-9 Model of flower development in rice.
(A) Modified ABC model in rice.
(B) Genes responsible for organ specification in rice and *Arabidopsis*.
ca, carpel; lo, lodicule; st, stamen; UO, unidentifiable organ.

Chapter 3

Introduction

Elucidation of the molecular mechanisms underlying flower and inflorescence development is one of the central issues in plant developmental biology. The ABC model that explains the principle of floral organ specification is a great milestone in flower development research, and a number of studies to understand further the detailed mechanisms of flower development have been performed based on this model (reviewed in Coen and Meyerowitz, 1991; Lohmann and Weigel, 2002; Prunet and Jack, 2014). Although floral shapes are diversified in angiosperms, the ABC model is applicable in principle to not only eudicot flowers but also monocot flowers. Among monocots, the molecular mechanisms of flower development are relatively well understood in rice (reviewed in Hirano et al., 2014; Tanaka et al., 2014; Yoshida and Nagato, 2011). Although class B genes specify stamen and lodicule (petal homolog), the *YABBY* gene *DROOPING LEAF* (*DL*), which is not included in the ABC model, plays a crucial role in carpel specification in rice (Nagasawa et al., 2003; Yamaguchi et al., 2004; Yao et al., 2008). These findings suggest that some modifications to the original ABC model are required to explain rice flower development.

In grasses such as rice and maize, floral organs are formed in a unique inflorescence unit, the spikelet (reviewed in Hirano et al., 2014; Tanaka et al., 2014; Yoshida and Nagato, 2011). The spikelet consists of floral organs such as lodicules,

stamens and carpels, and of organs specific to the spikelets such as a lemma, a palea, sterile lemmas and rudimentary glumes. This is in contrast with *Arabidopsis* flowers, which are generated directly on the inflorescence axis. Development and morphogenesis of the spikelet organs are regulated by many genes (reviewed in Hirano et al., 2014; Tanaka et al., 2014). For example, the *DEPRESSED PALEA1* (*DP1*) gene encoding an AT-hook DNA binding protein regulates proper development of the central region of the palea (Jin et al., 2011), whereas the *LONG STERILE LEMMA1* (*G1*) gene encoding a plant-specific nuclear factor specifies sterile lemma identity by repressing lemma identity (Yoshida et al., 2009). The *TRIANGULAR HULL1* (*TH1*) gene, belonging to the same gene family as *G1*, is involved in structural fine-tuning of the lemma and palea (Sato et al., 2014). Although *Arabidopsis* has homologs of these genes, there is no report that they are involved in flower development in *Arabidopsis*.

The arrangement of floral (spikelet) organs also differs between rice and *Arabidopsis*. Floral organs such as sepals, petals and stamens are formed in concentric whorls in *Arabidopsis*, and the size of each floral organ is similar (reviewed in Lohmann and Weigel, 2002; Prunet and Jack, 2014). Thus, *Arabidopsis* generates radially symmetric flowers. By contrast, in the rice spikelet, the lemma and palea, which are different in their morphology, are formed on the opposite sides in an alternating manner (reviewed in Hirano et al., 2014; Tanaka et al., 2014; Yoshida and Nagato, 2011). In addition, two lodicules are distributed asymmetrically on the lemma side of the spikelet (see below for details; Fig. 3-1 A, B, O). Thus, the rice spikelet displays bilateral symmetry with a single plane (transverse plane) along the lemma-palea axis. In

other words, the rice spikelet has polarity along the lemma-palea axis, which is associated with the potential to form different glumes (lemma or palea) and to initiate (or not to initiate) lodicules. Genetic regulation of floral symmetry is well studied in the flower of *Antirrhinum majus*, and several key genes responsible for dorsoventral asymmetry of the flower have been identified (reviewed in Busch and Zachgo, 2009; Preston and Hileman, 2009). However, our understanding of the mechanism of floral symmetry in monocots is poor.

Very long chain fatty acids (VLCFAs) are the fatty acids which have carbon (C) chain longer than 20. VLCFA has been thought to be the precursor of wax and cutin which constitute cuticle layer coating the aerial surface of plants (reviewed in Kunst et al., 2009). However, recent studies have revealed that VLCFA also plays important roles in plant development. VLCFA regulate vascular development and regeneration capacity as a signaling molecule in *Arabidopsis* (Nobusawa et al., 2013; Shang et al., 2016). The severe defect of VLCFA synthesis cause embryo or seedling lethality in *Arabidopsis* and rice, respectively (Bach et al., 2008; Ito et al., 2011).

Activation of long chain fatty acids (LCFA) and VLCFAs to their acyl-CoA derivatives is necessary for the synthesis of VLCFA. This reaction is catalyzed by long chain acyl-CoA synthetase (LACS), which is also involved in the transport of LCFA to endoplasmic reticulum (Jessen et al., 2015; reviewed in Lee and Suh, 2015). Thus, LACS is considered to be important for the biosynthesis of VLCFAs (reviewed in Kunst et al., 2009).

In this chapter, I focused on a new spikelet mutant, *two opposite lemma* (*tol*).

Although the *tol* mutant generated various abnormal spikelets, close examination suggests that these abnormalities are associated with the disruption of the polarity along the lemma-palea axis (transverse axis), and that the *tol* spikelet has two symmetry planes. Thus, the *tol* mutant should be good genetic material to elucidate the mechanism of spikelet symmetry in rice. I identified *RICE LACS1* (*RLA1*), the rice *LACS* gene, as one of the causes for the *tol* mutant phenotype. However, my analysis also demonstrated that the other mutation may be occurred in *tol* mutant and necessary for its phenotype.

Result

Structure of the wild-type spikelet in rice

In the wild-type spikelet, a lemma and a palea enclose the floral organs, such as lodicules, stamens and a pistil (Fig. 3-1 A, B, O) (reviewed in Hirano et al., 2014; Tanaka et al., 2014; Yoshida and Nagato, 2011). Two lodicules are formed asymmetrically only on the lemma side (Fig. 3-1 B, O). Although the lemma and palea are similar to each other at a glance, several differences are observed in their morphology (Ohmori et al., 2009). First, marginal regions are thick and curved inward in the lemma, while they are thin and mostly straight in the palea (Fig. 3-1 I, J). Second, the abaxial surface of the margin is rough in the lemma, while it is smooth in the palea. Third, the palea is formed in the same whorl as the lodicules, whereas the lemma is formed outside the palea whorl. The lemma and palea are formed in an alternate phyllotactic pattern such that lemma primordium initiates earlier than palea primordium. Because the lemma and palea thus differ in shape and the lodicules are located asymmetrically, the rice spikelet has only a single plane of symmetry (bilateral symmetry), along its transverse axis (Fig. 3-1 O).

Characteristic features of the spikelets in the *tol* mutant

The *tol* mutant showed several abnormalities in the lemma and palea. Because *tol* spikelet phenotypes are pleiotropic, I roughly classified them into three types: twin lemma (TL)-type, reduced lemma (RL)-type and loss of lemma (LL)-type.

The TL-type spikelet generated an extra lemma-like organ, which replaced the palea (Fig. 3-1 C, D). Observation of a cross section of the TL-type spikelet showed that this extra organ had thick and curled margins with a rough surface, suggesting that it corresponded to the lemma (Fig. 3-1 K, L). Two thin glume-like organs, named lateral glumes, were detected in the lateral region of the spikelet (Fig. 3-1 D, K, L). The lateral glumes had thin and straight margins, the surface of them was smooth (Fig. 3-1 L), and they were formed in the lodicule whorl (Fig. 3-1 D). These characteristics of the lateral glume are similar to those of the palea, suggesting that the lateral glume has partial identity with the palea. Two extra lodicules were also formed on the side of the extra lemma (Fig. 3-1 D). Thus, the number of lemmas and lodicules doubled. These observations suggest that, in the TL-type spikelet, the palea-side half of the spikelet was replaced by the lemma-like half of it, and two palea-like organs were ectopically formed in the lateral region. The overall arrangement of the spikelet organs (two lemmas and two lateral glumes) and floral organs suggests that the TL-type spikelet has two planes of symmetry, that is, is disymmetric.

I found that some TL-type spikelets had a thin and straight margin in the extra lemma (Fig. 3-1 M). This phenotype suggests that transformation of the palea into the lemma is incomplete. Thus, the TL-type spikelet was divided into two subtypes: a TLc-subtype spikelet with a complete extra lemma and a TLi-subtype spikelet with an incomplete extra lemma.

In the RL-type spikelet, a normal-looking lemma and a small organ opposite it were formed inside the sterile lemma (Fig. 3-1 E, F). The small organ had curled

margins and a rough surface at the abaxial side, suggesting that it had characteristics of the lemma (Fig. 3-1 N). A close-up view indicated that this small organ was initiated outside the normal lemma (Fig. 3-1 F). Therefore, the original lemma seems to be reduced to a small lemma-like organ (reduced lemma), whereas the normal-looking lemma is likely to be an ectopic lemma. In addition, two extra lodicules and two lateral glumes were formed in the RL-type spikelet, like the TL-type spikelet. These observations suggest that the RL-type spikelet is a modified version of the TL-type spikelet, in which the size of the original lemma is reduced.

In the LL-type spikelet, only one lemma-like organ was formed (Fig. 3-1 G). This organ was ectopically formed at the side where the palea would be in wild type, judging from the phyllotactic pattern. However, the original lemma and lodicules, which were formed opposite the ectopic lemma in the TL-type spikelet, were absent. Instead of the original lemma, the LL-type spikelet generated an extra sterile lemma (Fig. 3-1 H). Two lateral glumes were formed in the LL-type spikelet, as they were in the TL- and RL-type spikelets (Fig. 3-1 G). These phenotypes suggest that the LL-type spikelet is also a modified version of the TL-type spikelet, in which the development of the organs at the original lemma side was inhibited.

Taking these observations together, three spikelet types in the *tol* mutant showed partial similarity to each other. I propose that the RL- and LL-type spikelets are derived from the TL-type spikelet, arising from the duplication of the lemma-side half of the spikelet and extra formation of the palea-like lateral glumes. The frequency of each spikelet type is indicated in Table 3-1.

Analysis of the identity of the extra lemma by in situ hybridization

To check the identity of the extra lemma in TL-type spikelets and the putative reduced lemma in RL-type spikelets, I analyzed expression of the *DL* gene in these organs. *DL* is expressed in the central region of the leaf primordia and induces midrib formation in the leaf (Ohmori et al., 2011; Yamaguchi et al., 2004). In the spikelet, this gene was expressed in the region surrounding the midvein of the lemma (Fig. 3-2 A), as described previously (Toriba and Hirano, 2014). No expression was detected in the palea. Thus, *DL* is a good molecular marker to check lemma identity.

In situ analysis clearly indicated that *DL* was expressed in the extra lemma in TL-type spikelet (both TLc- and TLi-subtypes) (Fig. 3-2 B, C). *DL* was also expressed in the central region of the reduced lemma in RL-type spikelet (Fig. 3-2 D). These observations confirmed that the extra lemma of the TL-type spikelet and the reduced lemma of the RL-type spikelets had lemma identity.

Analysis of floral organs

Above analysis indicated that lemma and palea showed pleiotropic phenotypes in *tol* spikelet. Next, I investigated the analysis of flower organs.

In *tol* mutant, ectopic pistils were formed in whorl 3, in which stamens were also formed (Fig. 3-3 A, B). The ectopic pistils were morphologically abnormal: they looked like rod-like or palm-shaped. In particular, the palm-shaped pistils appeared to be formed from multiple carpel units, and the ovary walls were fused without forming a

bottle-like structure, unlike wild type (Fig. 3-3 B). Both types of pistil produced no ovules. In addition, the palm-shaped pistil was fused with a stamen at the edge of it (Fig. 3-3 C). The formation of ectopic pistils seems not to result from homeotic transformation, because normal stamens were also formed in whorl 3.

Organ fusion was often observed in the *tol* spikelets. For example, in a stamen, the filaments were fused and two anthers were formed on these fused filaments (Fig. 3-3 D). In some *tol* flowers, basal part of the pistil was larger than that of wild type (Fig. 3-3 E). Cross section revealed that the large pistil produced two ovules, whereas a single pistil produced one ovule in wild type (Fig. 3-3 G, H). Therefore, the large pistil seemed to be formed by the fusion of two pistils. In addition, the number of stigmas was increased. The formation of the fused organs may be associated with the defect in the establishment of border between flower organs, which might result from close proximity of floral organ primordia. Furthermore, chimeric organs were also observed in *tol* spikelets. A chimeric organ consisting of lodicule at the proximal part and anther at the distal part was generated in whorl 2, suggesting that the regulation of organ identity was affected (Fig. 3-3 F).

In addition to these morphological abnormalities, the orientation of the pistil was disturbed in *tol* spikelet. In wild type, the placenta was located on the palea side of the ovary (Fig. 3-3 G). By contrast, a single or two ovules were located on the side of one of lateral glumes in *tol* spikelets (Fig. 3-3 H, I). I examined the expression pattern of *DL*, the marker gene of the pistil. In wild type, *DL* was expressed in developing pistil except the palea side of the pistil (Fig. 3-3 J). In *tol* spikelets, *DL* expression was

detected in the pistil except the side of one of lateral glumes (Fig. 3-3 K). This result supported the disruption of the pistil orientation.

I next examined the number of stamens and pistils in *tol* mutants. The proportion of spikelets exhibiting increased stamen number was more than 60% among spikelets showing the *tol* phenotype, whereas such spikelets were about 10% in normal spikelets of the *tol* mutant (Fig. 3-3 L). This suggests that the regulation of normal development of the lemma/palea is associated with that of stamen number. In contrast to stamen number, pistil number was less affected in the *tol* mutant: the proportion of spikelets having more than two pistils was only a few percent in both the *tol*-type and normal spikelets (3.5 and 2%, respectively), suggesting that the *tol* mutation affects stamen and pistil development independently.

In summary, the morphological phenotypes of *tol* flower showed three types of defects: ectopic organ formation, organ fusion and chimeric organ formation. The abnormal pistil orientation may be associated with the overall arrangement of the flower organs in *tol*.

Analysis of developing spikelet by scanning electron microscopy

As described above, pleiotropic spikelet phenotypes were observed in the *tol* mutant. To know the developmental defects, I examined developing spikelets in wild type and *tol* using scanning electron microscopy (SEM).

In wild type, the flower meristem had a dome-shaped structure before initiation of stamen primordia (Fig. 3-4 A). In *tol* mutant, the flower meristem was

larger than that of wild type and this enlargement occurred along the lemma-palea axis, although the palea was replaced by the ectopic lemma in this spikelet (probably to develop into TL-type spikelet) (Fig. 3-4 C). In another spikelet, the abnormal morphology of the flower meristem was observed: some parts of the flower meristem appeared to be lacked in addition to an enlargement of the meristem (Fig. 3-4 D). Judging from the size and shape of the palea, this spikelet seems to be LL-type.

At the subsequent stage when stamen primordia initiated, the dome-shaped flower meristem initiated six stamen primordia, which is regularly arranged in the same whorl in wild type (Fig 3-4 B). In *tol* mutant spikelets, however, several abnormalities were observed (Fig. 3-4 E-G). First, the larger flower meristem initiated an increased number of stamens (Fig. 3-4 E). Second, the arrangement of the stamen primordia was disturbed: the initiation pattern of the primordia was irregular and was not formed in the same whorl (Fig. 3-4 F). Third, the size of the stamen was affected: in a case, the primordia were larger (Fig. 3-4 G), whereas they were smaller in another case (Fig. 3-4 F). In both cases, the flower meristem was enlarged and morphologically abnormal.

In summary, my observation of the spikelet at early developmental stage indicated that the flower meristem was enlarged and, in some case, morphologically abnormal, in the *tol* mutant. Probably due to the partial defects of the flower meristem, initiation pattern and size of the stamen primordia are seemed to be disturbed in the subsequent developmental stage.

Identification of the gene responsible for the *tol* mutation

To isolate the gene responsible for the *tol* mutation, I performed map-based cloning using F2 plants from a cross between *tol* (*japonica*) and Kasalath (*indica*). The result showed that the candidate gene for *tol* was located to within a 2.5-Mb region between the markers RM11412 and ss28 on the long arm of chromosome 1 (Fig. 3-5 A).

Next, I determined the whole genome sequence of *tol* by next generation sequencing. Comparison of the genomic DNA between *tol* and wild type demonstrated that an insertion of the DNA fragment was occurred in intron 13 of Os01g0681200 (LOC_Os01g48910), which resided in the mapping region (Fig. 3-5 B). Sequence analysis revealed that the inserted fragment was retrotransposon *Tos17* (Miyao et al. 2003) (Fig. 3-5 B). Except this insertion, I was not able to find any mutations that cause loss or reduction of protein function in the mapped region. Therefore, it is likely that Os01g0681200 (LOC_Os01g48910) was a candidate of the gene responsible for the *tol* mutant.

Os01g0681200 (LOC_Os01g48910) encodes a LACS protein, which has ATP-binding motif, linker domain and ACS signature motif (Fig. 3-5 C). LACS is involved in elongation of LCFA to generate VLCFAs (Lü et al. 2009). I designated Os01g0681200 as *RLA1* and the mutant allele of gene in the *tol* mutant as *rla-1-1*.

Relationships between *rla1* mutation and phenotype

To examine the effect of the mutation in *RLA1* on spikelet development, I searched other mutant alleles of *RICS LACS1* (*RLA1*) for *Tos17* mutant collections, and found three lines, in which *RLA1* had *Tos17* insertion (referred as *rla1-2*, *rla1-3* and *rla1-4*)

(Fig. 3-6 A). Morphological analysis of these mutants showed that some spikelets had two lemma and two lateral glumes (Fig. 3-6 B, C). Increase of the lodicules and stamens were accompanied with this type of phenotype. This phenotype was very similar to TL-type spikelet in the *tol* mutant. Another type of spikelets had defect in palea, which was smaller than that of wild type and was divided into two parts (Fig. 3-6 D, E). These divided palea was similar to lateral glumes. This spikelet phenotype resembled LL-type spikelet. Taking together, abnormal spikelets in *RLA1* single mutants were similar to the spikelets observed in the *tol* mutant as described in Fig. 3-1.

I next analyzed the frequency of the abnormal spikelets in each *RLA1* single mutant (Table. 3-2). The result showed that abnormal *tol*-like spikelets in *rla1-2*, *rla1-3* and *rla1-4* were obviously fewer than those of the *tol* mutant, suggesting that the spikelet phenotypes and their frequency observed in *tol* were not simply explained by a single mutation occurring in the *RLA1* gene.

To examine whether *rla1-1* mutation is responsible for *tol* phenotypes, the relationship between the genotypes of *RLA1* and *tol* phenotypes was analyzed using F2 plants from a cross between *tol* and Kasalath (Table. 3-3). As a result, all plants which showed *tol* spikelet phenotypes were homozygous for *rla1-1*. However, some plants homozygous for *rla1-1* did not show *tol* phenotype, suggesting that a mutation other than *rla1-1* is involved in this phenotype.

In summary, it is possible that *rla1-1* is one of the causes for the *tol* mutant phenotype, but the whorl picture of *tol* mutation could not simply explained by the *rla1-1* mutation alone.

Discussion

Spikelet and flower phenotypes in the *tol* mutant

In this chapter, I analyzed spikelet phenotypes in the *tol* mutant. *tol* spikelets showed pleiotropic phenotypes not only in the shape and arrangement of the lemma and palea (spikelet organs) but also in those of the flower organs such as stamens and pistils. I observed the spikelet phenotypes and classified them into three types. According to this classification, the morphological analysis suggests that pleiotropic spikelet phenotypes are continuous and are derived from a primary defect observed in the TL-type spikelet. This primary defect can be regarded as the duplication of the lemma-side half of the spikelet, with successive reduction in the number of cells on the original lemma side giving rise to reduction or loss of the original lemma and lodicules. Because of the duplication of the lemma-side half, the TL-type spikelet acquires a new plane of symmetry, the medial plane, which is perpendicular to the transverse plane. This suggests that the putative gene responsible for the *tol* mutation is involved in polar pattern formation along the transverse axis.

In general, the number of floral organs increases in the mutant, in which the floral meristem is enlarged. In the *tol* spikelets, the number of lemmas, paleas/palea-like organs and lodicules was increased. Stamen number was also increased to some extent. Thus, it seems likely that defects in the regulation of the number of spikelet and flower organs in the *tol* mutant result from an enlargement of the spikelet/flower meristem. Supporting this idea, the observation by SEM indicated that the flower meristem of *tol*

was enlarged,

Irregular activity of the spikelet and flower meristem in the *tol* mutant

Based on the idea that *tol* spikelet formation is associated with meristem size, I propose a model that accounts for the three types of *tol* spikelets (Fig. 3-7). I found that the spikelet meristem was enlarged from initial stages of spikelet development. The enlargement of the meristem may be associated with the loss of polarity along the transverse axis and may change the spikelet shape from monosymmetry to disymmetry. The abnormal pistil orientation observed in *tol* spikelets may be associated with this loss of polarity. Space for the initiation of extra organs would be sufficient in this enlarged meristem. Whereas the lemma and the lodicules could be formed on both sides, palea-like organs would be initiated in the lateral side of the meristem. Thus, the TL-type spikelet may be formed. An observation by SEM showed that, in some case, the *tol* flower meristem appeared to be partly lacked in addition to its enlargement. In such flower meristems, the activity of the meristem to supply cells for lemma and lodicule development may be reduced at the original lemma side. Thus, the RL- and LL-type spikelets would result from this partial inactivation of the meristem.

A mutation in the rice *FLORAL ORGAN NUMBER1* (*FON1*) or *FON2* gene causes an enlargement of the meristem, resulting in an increase in the number of floral organs, such as pistils and stamens (Suzaki et al., 2004; Suzaki et al.,2006). *FON1* and *FON2* are orthologs of *Arabidopsis CLAVATA1* (*CLV1*) and *CLV3* (Clark et al., 1997; Fletcher et al., 1999; reviewed in Ha et al., 2010). Both the *FON* and *CLV* genes

negatively regulate stem cell proliferation, and plants having defects in these genes show a stronger increase in pistil number than in stamen number. By contrast, pistil number was less affected in the *tol* mutant than stamen number. Therefore, roles in meristem size regulation may be different between the *tol* and *fon* mutants: a failure in meristem size regulation seems to occur at an early stage of spikelet development in the *tol* mutant and may be caused by a defect in an unknown mechanism, which is unrelated to the regulation of stem cell proliferation. Apart from this difference, the *fon1* and *fon2* mutants exhibit spikelets similar to the TL-type spikelet at a low frequency (Suzaki et al., 2004; unpublished observations performed in my laboratory). This fact supports the idea that the formation of the TL-type spikelet is associated with meristem size.

The genetic mechanism underlying floral symmetry is well understood in *Antirrhinum*. Several genes responsible for either dorsal or ventral identity and their coordinated action specify the asymmetric flower in *Antirrhinum* (reviewed in Busch and Zachgo, 2009; Preston and Hileman, 2009). Floral asymmetry in *Antirrhinum* is mainly related to the size and shape of petals. Although the number of petals and normal stamens is increased in the *Antirrhinum cycloidea* (*cyc*) mutant, rearrangement of the floral organs does not occur (Luo et al., 1996). By contrast, the number of flower and spikelet organs was increased in the rice *tol* mutant, and their arrangement was altered: the lemma and lodicule were formed on the side where the palea is formed in wild type, and the palea-like organs were initiated at the lateral regions. Therefore, disruption of asymmetric patterning of the flower/spikelet seems to be different between these rice and *Antirrhinum* mutants. Isolation of the gene responsible for the *tol* mutation and

elucidation of its function should reveal a new mechanism underlying the regulation of flower/spikelet symmetry.

Abnormal organization of the flower meristem in the *tol* mutant

In *superwoman1* (*spw1*) mutant, in which one of class B MADS-box gene was defective, ectopic pistils were formed in whorl 3 at the expense of stamen formation (Nagasawa et al., 2003; Chap 2 in this thesis). In some *tol* flower, the ectopic pistil was formed in whorl 3, but normal shaped stamens were also formed in this region. Therefore, the ectopic pistil in *tol* seems to be formed by the mechanism different from homeotic transformation observed in *spw1*. One possibility is that the boundary between whorl 3 and whorl 4 might be ambiguous in *tol* flowers, resulting in the invasion of pistil formation activity into whorl 3. The idea that the boundary is not properly determined is supported by the SEM observation that the stamen primordia were not formed in the same whorl in developing *tol* flower. The fused organs, such as stamen-stamen or stamen- pistil, were found in the *tol* flower. These fused organs are considered to be caused by an ambiguous boundary between organ primordia. The disturbed arrangement of the primordia observed by SEM may be associated with this organ fusion. Taken together, the formation of ectopic organ and fused organ might result from defects in the flower meristem in *tol*, namely, failures in the proper establishment of the boundaries between whorls or those between organ primordia. In other words, the organization of the flower meristem might be disturbed in the *tol* mutant.

The *tol* mutant has a mutation in the gene encoding LACS.

The map-based cloning and the next generation sequencing suggested that the *tol* mutant has a mutation in *RLA1*, a rice *LACS* gene. It is possible that the insertion of *Tos17* into intron 13 prevents efficient splicing of the precursor of *RLA1* transcript, resulting in the reduction in the level of the mature transcript. The single mutants of *RLA1* (*rla1-2*～*rla1-4*) showed *tol*-like spikelet phenotypes despite low frequency of their appearance, suggesting that *rla1* mutations may be associated with the mutant phenotype. Among *rla1* single mutants, the frequency of the appearance of *tol*-like spikelet was the higher in *rla1-2* (insertion in exon 3) than in *rla1-3* and *rla1-4* (insertion in intron 12 or 3' UTR). This result also supports the idea that the mutation in *RLA1* is a possible cause of the *tol* mutant.

RLA1 encodes a LACS protein, which activates LCFAs to their acyl-CoA derivatives which is utilized for synthesis of VLCFAs (reviewed in Bach and Faure, 2010). *Arabidopsis* has 9 *LACS* genes and their functions are partially redundant, although their specificity of the substrate and the expression pattern are diverse (Shockey et al., 2002). I found 10 *LACS* genes in the rice genome. It seems likely the low frequency of the abnormal spikelets in *rla1* single mutants results from the redundancy in rice *LACS* genes.

VLCFA is required for meristem activity.

A mutation in the rice *ONION1* (*ONI1*) and *ONI2* gene lead seedling-lethal phenotypes

(Ito et al., 2011; Tsuda et al., 2013). *ONI1* and *ONI2* encodes β-ketoacyl CoA synthase which is important for the synthesis of VLCFAs. In fact, the amount of VLCFAs is reduced in *oni1* and *oni2* mutant. *oni1* mutants showed the degeneration of the SAM, in addition to disturbed epidermal structure (Ito et al., 2011). *oni2* showed the disturbed epidermal structure and fused leaves (Tsuda et al., 2013). These findings indicate that VLCFAs are essential for meristem maintenance and proper organ formation in rice. In this study, I observed that the flower meristem was partially disorganized and some floral organs were fused in the *tol* mutant. Therefore, these abnormality in *tol* spikelet seems to be associated with reduction in VLCFA content. Further studies should be performed to determine whether the amount of VLCFAs is decreased in the *tol* mutant.

The relationships between the *RLA1* genotypes and the *tol* spikelet phenotypes using F2 plants from a cross between *tol* (*japonica*) and Kasalath (*indica*) indicated that *tol* has a mutation in a gene other than *RLA1*. The identification of the second gene responsible for the *tol* spikelet phenotype is necessary to reveal the mechanisms of spikelet development. I have tried to isolate the second gene by a map-based cloning strategy. However, probably due to low expressivity of the *tol* spikelet phenotype in Kasalath background, I failed to identify the mutation related to the phenotype. In future, it is possible that I will identify the second gene responsible for the *tol* phenotype by using another method, such as MutMap using F2 plants between *tol* and a japonica strain (Abe et al., 2012).

Table 3-1. Frequency of spikelet types in the *tol* mutant

phenotype	No. of spikelet	percentage (%)
TL-type	78	31.8
Tc-subtype	(56)	
Ti-subtype	(22)	
RL-type	60	24.5
LL-type	7	2.9
Normal	100	40.8
Total	245	100

'Normal" means the *tol* spikelet without any abnormality in the lemma and palea.

Table 3-2 Frequency of abnormal spikelets in *rla1* mutants

mutant line	the number of spikelets observed	the number of *tol*-like spikelet	the frequency of *tol*-like spikelet (%)
rla1-2	560	23	4.1
rla1-3	1176	20	1.7
rla1-4	715	1	0.1
tol	245	145	59.3

Table 3-3 Relationship between the genotypes of *RLA1* and *tol* phenotypes

	rla1-1/rla1-1	*RLA1/rla1-1*	*RLA1/RLA1*	total
tol-like phenotype	26	0	0	26
unifentifiable phenotype	19	24	0	43
wild-type phenotipe	32	168	91	291
total	77	192	91	360

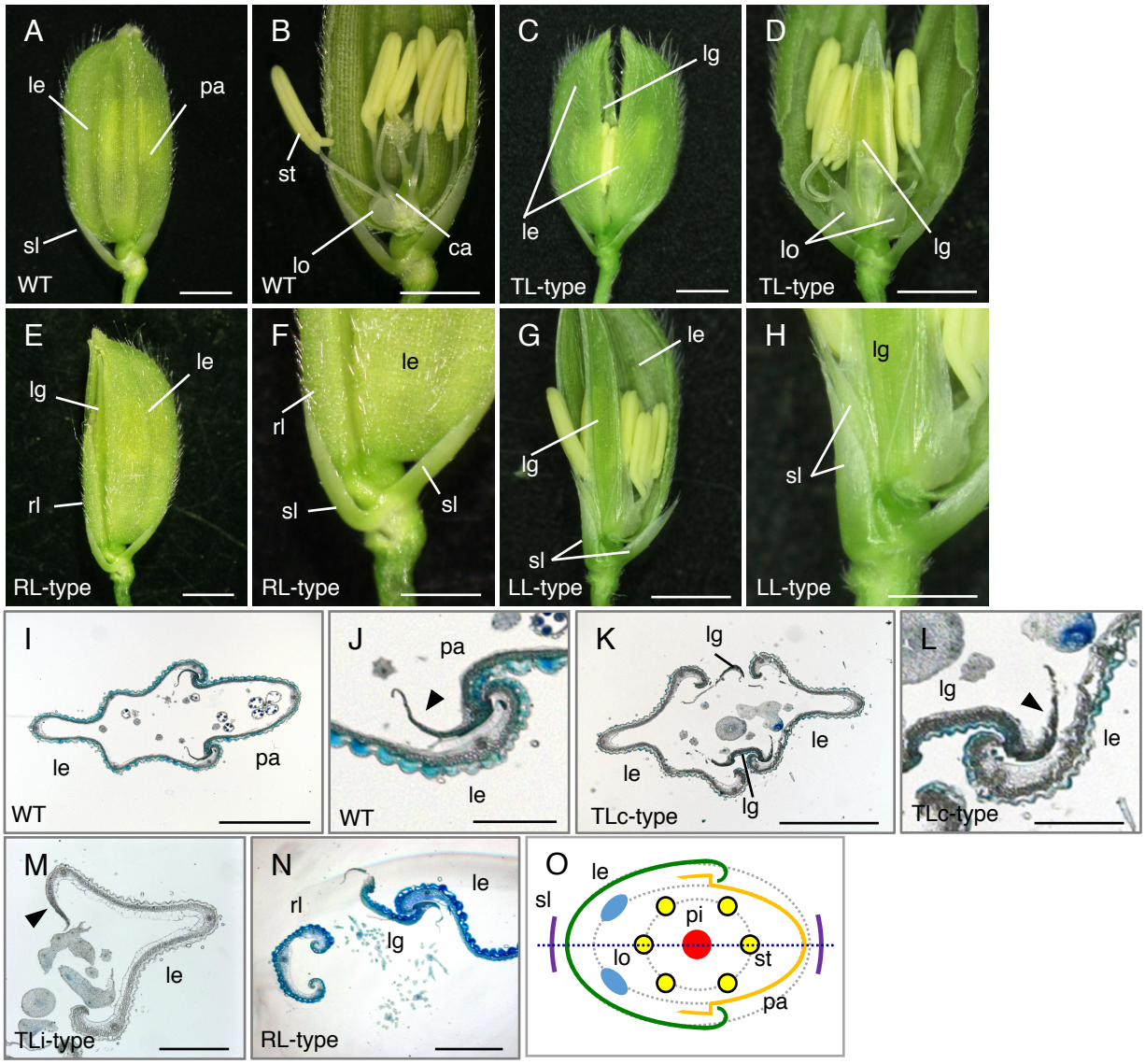

Fig. 3-1 Spikelet phenotypes in the *tol* mutant.
(A, B) A wild-type spikelet.
(C, D) A TLc-type spikelet of the *tol* mutant.
(E, F) An RL-type spikelet of the *tol* mutant.
(G, H) An LL-type spikelet of the *tol* mutant. Part of the lemma and palea are removed in (B, D, G, H).
(I, J) A cross section of a wild-type spikelet. A close-up view of the marginal regions of the lemma and palea are shown in (J). The arrowhead indicates the thin margin of the palea.
(K, L) A cross section of the TLc-type spikelet. Close-up view of the marginal regions of the lemma and lateral glume is shown in (L). Arrowhead indicates a thin and straight margin of the lateral glume.
(M) A cross section of the ectopic lemma of TLi-type spikelet. Arrowhead indicates a thin and straight margin of the ectopic lemma.
(N) A cross section of part of the RL-type spikelet. The reduced lemma (rl) side is shown.
(O) Schematic representation of the wild-type spikelet. Green and orange indicate the lemma and the palea, respectively. The horizontal broken line indicates a plane of symmetry. Gray broken lines indicate concentric whorls.
le, lemma; lg, lateral glume; lo, lodicule; pa, palea; pi, pistil; rl, reduced lemma; sl, sterile lemma; st, stamen. Scale bars = 2 mm in (A-E, G, I, K), 1 mm in (F, H, M, N), 0.5 mm in (J, L).

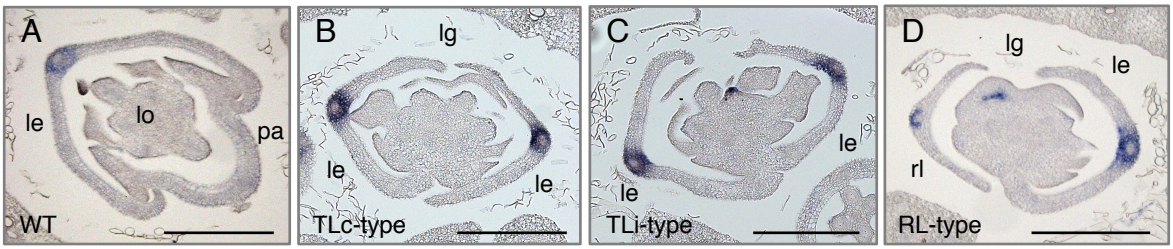

Fig. 3-2 In situ hybridization analysis of *DL* expression in developing spikelets.
(A) A wild-type spikelet.
(B) A TLc-type spikelet of the *tol* mutant.
(C) A TLi-type spikelet of the *tol* mutant.
(D) An RL-type spikelet of the *tol* mutant.
le, lemma; lg, lateral glume; lo, lodicule; pa, palea; rl, reduced lemma. Scale bars = 80 μm.

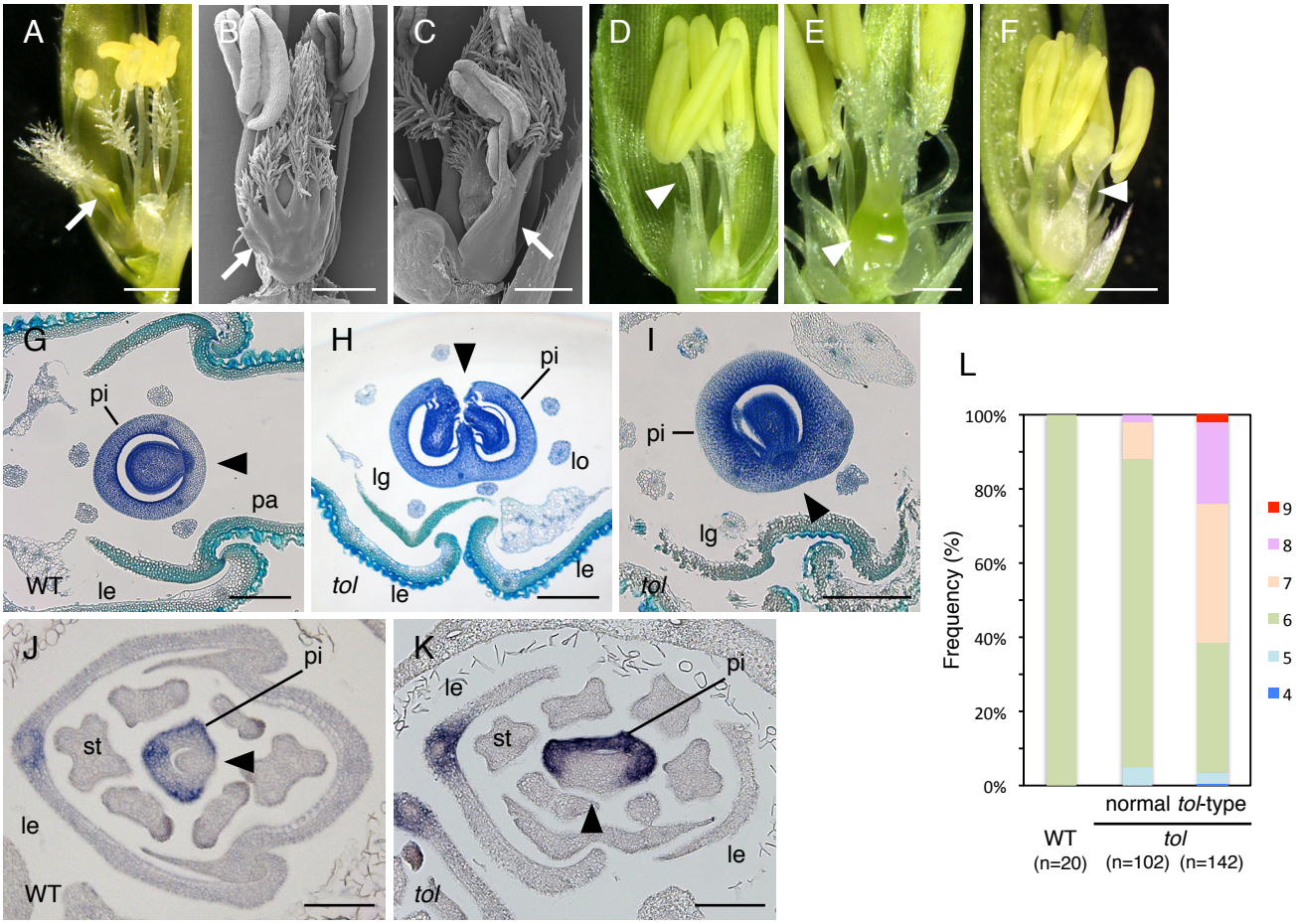

Fig. 3-3 Flower phenotypes in the *tol* mutant.
(A, B) Spikelets producing ectopic pistils in whorl 3: (A) a rod-like pistil, (B) palm-shaped pistils. The white arrow indicates the ectopic pistil.
(C) A stamen (white arrow) fused with the palm-shaped pistil.
(D) The stamen, in which two anthers were formed in the top of the fused filaments (white arrowhead) (stamen-stamen fusion).
(E) An enlarged pistil (white arrowhead).
(F) The chimeric organ consisting of the lodicule- and anther-like structure (white arrowhead).
(G-I) Cross sections of the pistils of the mature spikelet in wild type (G) and *tol* mutant (H, I). The enlarged and the normal pistil generated two ovules (H) and one ovule (I), respectively.
(J, K) In situ hybridization of *DL* in developing spikelets of wild type (J) and *tol* (K).
The black arrowheads indicate the placenta
(L) Frequency of the number of stamens in wild type and *tol* mutant spikelets. "Normal" means *tol* spikelets without any abnormality in the lemma or palea. "*tol*-type" includes TL-, RL- and LL-type spikelets.
le, lemma; lg, lateral glume; lo, lodicule; pa, palea; pi, pistil; st, stamen. Scale bars = 1 mm in (A, D, F), 500 μm in (B, C, E), 250 μm (G, H, I) and 100 μm (J and K).

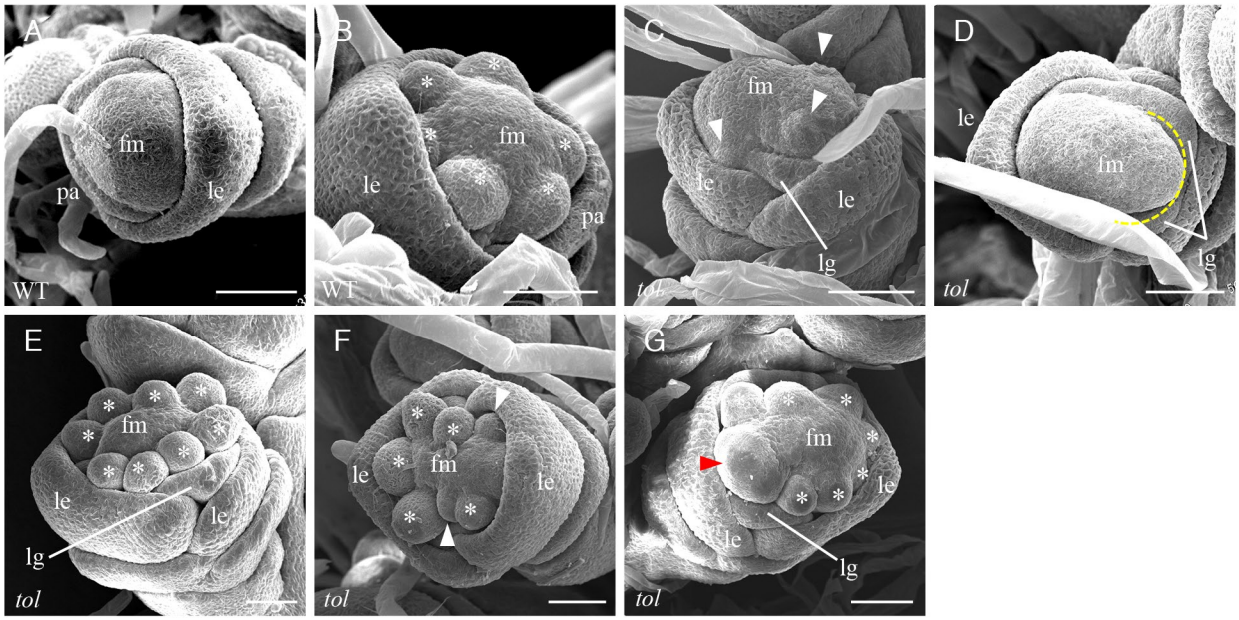

Fig. 3-4 Phenotypes of developing spikelets in the *tol* mutant.
(A, B) SEM images of the developing spikelet just before (A) and after (B) initiation of stamen primordia in wild type.
(C, D) SEM images of the developing spikelet before initiation of stamen primordia in *tol*. Abnormal bulges were observed in enlarged flower meristem in (C) (white arrowheads); some parts in the enlarged flower meristem were lacked (D).
(E-G) SEM images of the developing spikelet after initiation of stamen primordia in *tol*. The spikelets showed an increased number of the stamen primordia (E), an abnormal arrangement of the stamen primordia (F) and an enlargement of the stamen primordium in addition to an increase of stamen primordia (G). White and red arrowhead indicate the smaller and the larger stamen primordia, respectively.
fm, flower meristem; le, lemma; lg, lateral glume; pa, palea. Asterisks indicate stamen primordia. Scale bars = 50 μm.

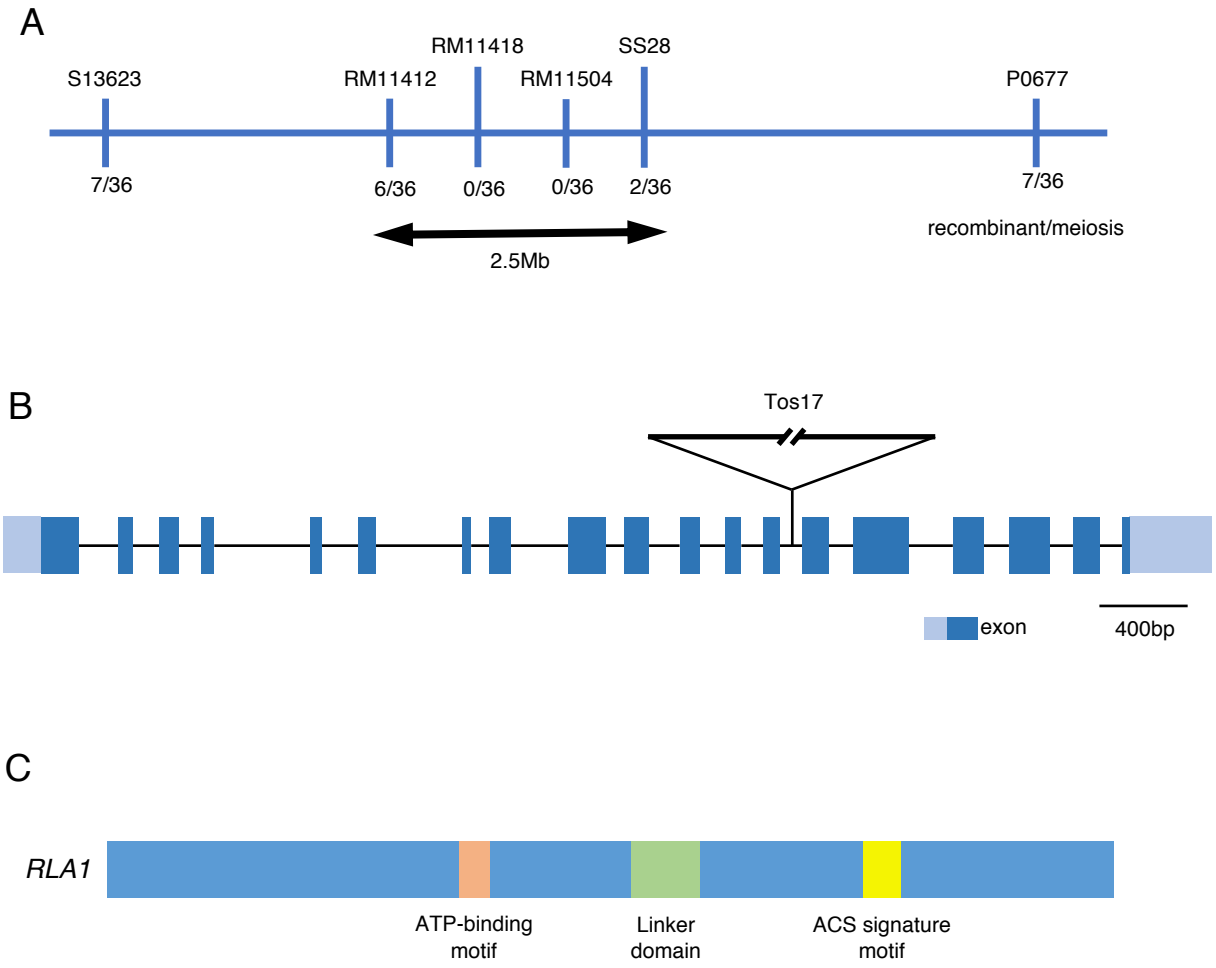

Fig. 3-5 Mapping and identification of the mutation responsible for *tol* phenotype.
(A) Rough mapping of *tol* mutation.
(B) Schematic representation of the *RLA1*gene and the position of the *Tos17* insertion in *tol* mutant. Blue boxes indicate exons (light blue, UTRs), and solid lines indicate introns.
(C) Schematic representation of the *RLA1* protein. The ATP-binding motif, linker domain and ACS signature motif are indicated by orange, green and yellow boxes, respectively.

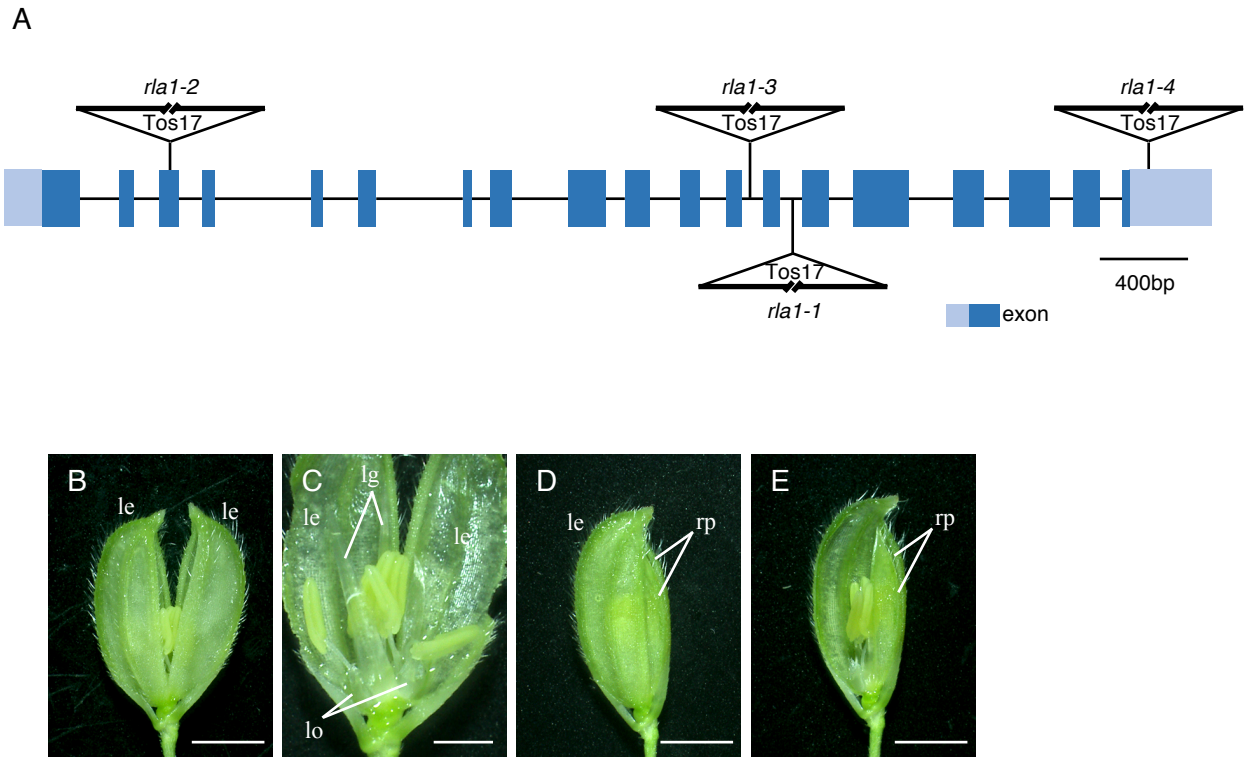

Fig. 3-6 Spikelet phenotypes in the *rla1* single mutants.
(A) Schematic representation of the position of the *Tos17* insertion in *rla1-1* (*tol* mutant), *rla1-2*, *rla1-3* and *rla1-4* mutants. Blue boxes indicate exons (light blue, UTRs), and solid lines indicate introns.
(B, C) A spikelet with two lemma and two lateral glumes in the *rla1-2* mutant.
(D, E) A spikelet with reduced and split palea. The lemmas are partially removed in (C, E).
le, lemma; lg, lateral glume; lo, lodicule; rp, reduced palea. Scale bars = 2 mm in (B, D, E) and 1 mm in (B).

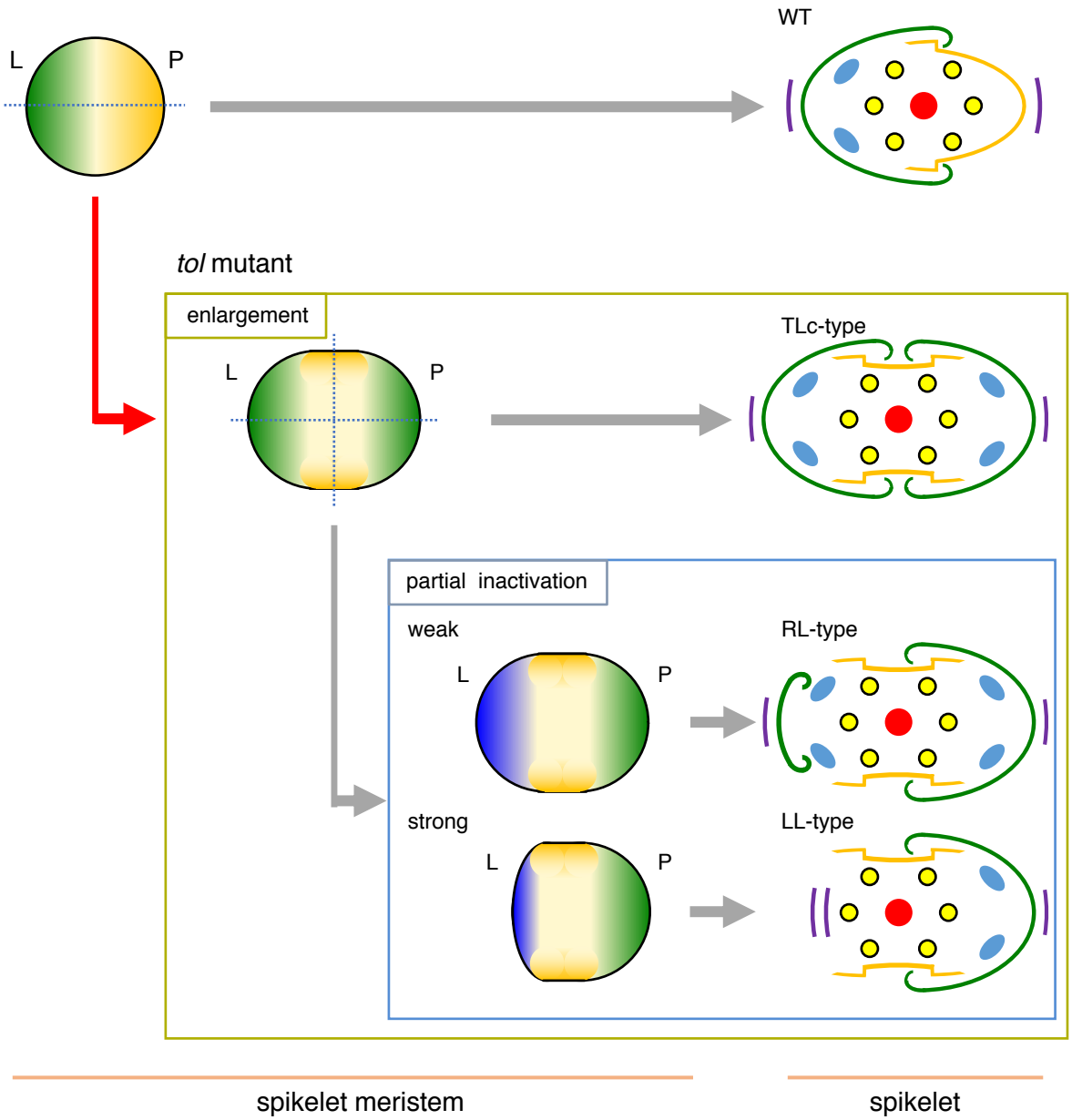

Fig. 3-7 A model of *tol* spikelet formation.
Green and orange areas in the meristem indicate the regions where organs with lemma and palea identity, respectively, are initiated. The blue area indicates the region where meristematic activity is partially reduced in the RL- and LL-type spikelets. Broken lines indicate planes of symmetry. L and P indicate the lemma side and the palea side, respectively.

Chapter 4

Materials and Methods

Plant materials

All rice strains used in this study were *Oryza sativa* spp. *japonica*, except Kasalath, *Oryza sativa* spp. *indica*. The *osmads58-7* mutant was isolated by Dr. Y. Yasui using the TILLING method from the mutant collections maintained by the National Bio-Resource Project (Satoh et al., 2010; Suzuki et al., 2008). *osmads58-7* has a point mutation at the 5' splice site of intron 1 (Fig. 2-1 in Chap 2), which should lead to mis-splicing of mRNA. *spw1-11* was identified from a *Tos17* mutant collection by Dr. W. Tanaka (Miyao et al., 2007). *spw1-11* has a 4767-bp deletion including the last two exons of *SPW1*. *osmads3-fe1*, *fon2-3*, and *dl-sup1* have been described by Yasui et al., (2017), Suzaki et al., (2006), and Yamaguchi et al., (2004), respectively. The *tol* mutant was identified among mutants that had been roughly selected from the *Tos17* mutant panel (Miyao et al., 2007) and maintained in my laboratory. *rla1-2*, *rla1-3* and *rla1-4* were identified as the mutants, in which the retrotransposon *Tos17* is inserted in *RLA1*, from the *Tos17* mutant panel. Taichung65 (T65) and Nipponbare were mainly used as a control (wild type) for comparing phenotypes, SEM, and in situ hybridization.

Generation of an *OsMADS58* knockout line by CRISPR/Cas9

To generate an *OsMADS58* knockout line, a 20 bp-sequence near the 5' end of the

K-box was selected as a target site for the guide RNA (gRNA) (Fig. 2-1 in Chap 2). Synthetic oligonucleotides consisting of the target sequence and an adaptor sequence were annealed to make a double-stranded DNA fragment (The primers are listed in Table. 4-1). This fragment was ligated into the gRNA cloning vector pU6gRNA-oligo, which was linearized by *Bbs*I (Mikami et al., 2015). The OsU6 promoter and gRNA sequence were then excised from the pU6gRNA-oligo vector and inserted into the *Asc*I and *Pac*I sites of pZH_OsU3gYSA_MMCas9. This recombinant plasmid was introduced into *Agrobacterium tumefaciens* strain EHA101 and transformed into calli by the method of Hiei et al. (Hiei et al., 1994). The nucleotide sequence of the target site in regenerated plants was verified by sequencing (The primers are listed in Table. 4-1).

Morphological observation

Phenotypes of flowers just before heading and one month after heading were observed. Photographs were taken by using an SZX10 stereoscopic microscope and DP22 or DP21 camera (Olympus).

For SEM analysis, samples were fixed in 4% paraformaldehyde and 0.25% glutaraldehyde in 0.1 M sodium phosphate buffer, pH 7.2, at 4°C for 24 h. The fixed samples were dehydrated in a graded ethanol series. After ethanol was replaced with 3-methylbutyl acetate, the samples were dried at the critical point and sputter- coated with platinum. For observation, a scanning electron microscope (model JSM-820S; JEOL) was used at an accelerating voltage of 5 kV.

Histological observation and in situ hybridization

Developing spikelets just before heading were fixed and dehydrated, as described above. After ethanol was replaced with xylene, the samples were embedded in Paraplast Plus (McCormick Scientific, St. Louis, MO), and sectioned at 8-μm thickness by a rotary microtome. The sections were mounted on glass slides and stained with 0.05% toluidine blue-O for observation by light microscopy.

To generate probes for in situ hybridization, partial cDNA fragments were amplified from the genes by PCR (The primers are listed in Table. 4-1). The fragment of *OsMADS15* was inserted into the pCRII-TOPO vector (Invitrogen, Carlsbad), whereas that of *OsMADS13*, *SPW1*, and *OsMADS3* was inserted into the pCRII vector (Invitrogen, Carlsbad). RNA probes were transcribed by using T7 or SP6 RNA polymerase and labeled with digoxigenin (Roche, Mannheim). *OSH1* and *DL* probes were prepared as described previously (Sato et al., 1996; Yamaguchi et al., 2004). In situ hybridization and immunological detection of the hybridized transcripts were performed as described by Toriba and Hirano (2018). A BX50 optical microscope (Olympus, Tokyo) and an Axio Cam 506 color camera (Carl Zeiss, Oberkochen) were used for observation.

Map-based cloning and next generation sequencing

F2 plants from a cross between *tol* (*japonica*) and Kasalath (*indica*) were used for mapping. The locus responsible for the *tol* mutant phenotype was mapped to a region between SSR marker RM11412 (25.9 Mb) and SCAR marker ss28 (28.5 Mb) on

chromosome 1. ss28 primer is listed in Table 4-1.

Next generation sequencing of genomic DNA of *tol* was performed in collaboration with Dr. T. Kurata and Dr. T. Sakamoto (NAIST). A kit, Mate Pair Library v2 (illumina), was used for construction of a genomic fragment DNA library. The genome DNA was cut into fragments using S220 Focused-ultrasonicators (Covaris). For quantification of library, KAPA Library Quantification Kits (KAPA) was used. Single reads of 75 bp were obtained from GAIIx (Illumina). Extracted FASTQ data were imported into StrandNGS software (Strand Life Science, Inc). They are assembled with the reference genome sequence (IRGSP_1.0) in StrandNGS by using the COBweb program. The BAM file was exported from Strand NGS, and the mutations which was located in delimited region by map-based cloning was elucidated using the IGV genome browser (BROAD Institute).

Analysis of relationships between the *rla1* mutation and the *tol* phenotype

F2 plants from a cross between *tol* (*japonica*) and Kasalath (*indica*) were used for the comparison of *RLA1* genotype and the *tol* phenotype. Genotyping of *rla1-1* was performed by 3-primer PCR genotyping using the primer sets listed in Table 4-1. A pair of primers was used to amplify 623-bp fragments from the wild-type genome, whereas the other pair of primers was used to amplify 398-bp fragments from the *rla1-1* genome.

Table. 4-1 PCR primers used in this study

Guide RNA sequence for *OsMADS58* knockout by CRISPR/Cas9	
OsMADS58-guideRNA d1	GTTGATTGATCTCTGCAACTGTAC
OsMADS58-guideRNA u2	AAACGTACAGTTGCAGAGATCAAT
Sequencing ofthe CRISPR/Cas9 target site in *OsMADS58*	
OsMADS58-sequence d1	ATTGTTTAGAAAATGAAAGGTGG
OsMADS58-sequence u2	GGAATTTCCATTGTGTAAAGC
Probe preparation for *OsMADS15*	
OsMADS15-in situ probe d1	GCACTTCTTCCACCACAAAA
OsMADS15-in situ probe u2	GCAGCAGGCAAACACATATAT
Probe preparation for *OsMADS13*	
OsMADS13-in situ probe d1	AGATTGAGCTTCAGAACGAC
OsMADS13-in situ probe u2	AGCCACATCAGTAGTGTCTGTC
Probe preparation for *SPW1*	
SPW1-in situ probe d1	TTGGATCGAGCAGTATGAGAATATGC
SPW1-in situ probe u2	TATCAACCGAGGCGCAGG
Probe preparation for *OsMADS3*	
OsMADS3-in situ probe d1	TATGCTGAAGTTGAGTACATGC
OsMADS3-in situ probe u2	GCCTAATGACAATACTGGTTATG
Mapping marker ss28	
ss28 d1	TTTTTCCGATTAAAACCTCC
ss28 u2	AGAGAGAGACAAGGGCATAG
3-primer PCR genotyping for *rla1-1*	
rla1-genotyping d1	ATCCATCGACTAAAACTTCC
rla1-genotyping d2	TGGAGCAGTGGATAAATATG
rla1-genotyping u3	GAAAGGAAGCAAGCATGAAG

Chapter 5

Conclusion and perspective

The mechanisms of flower development are basically conserved among angiosperms. By contrast, they are also diverse depending on the plant species. To understand the diverse mechanisms of flower development in angiosperms, developmental studies in various species are necessary. In this thesis, I studied the mechanisms of spikelet and flower development focusing in rice. I obtained some insights to understand the mechanisms underlying flower and spikelet development in relation to meristem function in rice, and revealed gene function unique to this plant.

In chapter 2, I focused on the mechanisms regulating carpel specification and flower meristem determinacy. I revealed that carpel identity is specified in the absence of the rice class C genes, *OsMADS3* and *OsMADS58*, and is not specified in the presence of them alone. From these results, I concluded that class C genes are not a key regulator for carpel specification in rice. As described previously in the paper from my laboratory (Yamaguchi et al., 2004), carpel identity is likely to be specified by the *YABBY* gene *DROOPING LEAF* (*DL*). In addition, I revealed that *DL* plays an important role in flower meristem determinacy.

In chapter 3, I focused on the *two opposite lemma* (*tol*) mutant, which showed the pleiotropic phenotypes in both spikelet and flower organs. These phenotypes resulted from the irregular regulation of the spikelet and flower meristem. I revealed

that *RICE LACS1* (*RLA1*), which is involved in the synthesis of very long chain fatty acids (VLCFAs), is partially responsible to the *tol* phenotype.

Flower and spikelet development

I showed that, although *DL* is required for carpel specification, it is not sufficient to complete pistil morphology, which is consisted of the stigma, style, ovule, and ovary. The mechanism underlying the construction of these structures and the gene functions responsible for pistil morphogenesis are poorly understood in rice. This situation is highly contrast with the deep understanding of the mechanisms and the gene functions in regulating pistil morphogenesis in *Arabidopsis* (Eshed et al., 2001; Kuusk et al., 2002; Liljegren et al., 2000). It is likely that the cooperation of *DL* and class C genes are required for the elaboration of complete pistil morphology. A large number of genes would be regulated by *DL* and class C genes independently or cooperatively. In future, it will be essential to identify the genes regulated by *DL* and class C genes and to reveal the mechanism how *DL* and class C genes cooperatively regulate the elaboration of pistil morphology.

The flower and spikelet are bilateral symmetry in rice, whereas the flower is radial symmetry in *Arabidopsis*. It is of great interest to understand how the polarity is established along symmetry axis and how flower and spikelet organs were arranged and differentiated along this polarity.

VLCFA and meristem regulation

My study suggests that VLCFAs seems to be involved in the regulation of meristem activity and organization of the meristem in rice. In *Arabidopsis*, VLCFAs reportedly act as signaling molecules and regulate the activity of the shoot apical meristem and the induction of the lateral root meristem (Nobusawa et al., 2013; Shang et al., 2016). However, the function of VLCFAs in the regulation of the flower meristem remains unrevealed not only in rice but also in *Arabidopsis*. Thus, the study to elucidate the functions of VLCFAs may reveal the new pathways to regulate flower development.

References

Abe, A., Kosugi, S., Yoshida, K., Natsume, S., Takagi, H., Kanzaki, H., Matsumura, H., Yoshida, K., Mitsuoka, C., Tamiru, M., Innan, H., Cano, L., Kamoun, S., and Terauchi, R. (2012). Genome sequencing reveals agronomically important loci in rice using MutMap. Nat Biotechnol **30,** 174-178.

Alvarez, J., and Smyth, D.R. (1999). *CRABS CLAW* and *SPATULA*, two *Arabidopsis* genes that control carpel development in parallel with *AGAMOUS*. Development **126,** 2377-2386.

Bach, L., and Faure, J.D. (2010). Role of very-long-chain fatty acids in plant development, when chain length does matter. C R Biol **333,** 361-370.

Bach, L., Michaelson, L.V., Haslam, R., Bellec, Y., Gissot, L., Marion, J., Da Costa, M., Boutin, J.P., Miquel, M., Tellier, F., Domergue, F., Markham, J.E., Beaudoin, F., Napier, J.A., and Faure, J.D. (2008). The very-long-chain hydroxy fatty acyl-CoA dehydratase PASTICCINO2 is essential and limiting for plant development. Proc Natl Acad Sci USA **105,** 14727-14731.

Becker, A., and Theissen, G. (2003). The major clades of MADS-box genes and their role in the development and evolution of flowering plants. Mol Phylogenet Evol **29,** 464-489.

Bowman, J.L., and Smyth, D.R. (1999). *CRABS CLAW*, a gene that regulates carpel and nectary development in *Arabidopsis*, encodes a novel protein with zinc finger and helix-loop-helix domains. Development **126,** 2387-2396.

Bowman, J.L., Smyth, D.R., and Meyerowitz, E.M. (1991). Genetic interactions among floral homeotic genes of *Arabidopsis*. Development **112,** 1-20.

Busch, A., and Zachgo, S. (2009). Flower symmetry evolution: towards understanding the abominable mystery of angiosperm radiation. Bioessays **31,** 1181-1190.

Cartolano, M., Castillo, R., Efremova, N., Kuckenberg, M., Zethof, J., Gerats, T.,

Schwarz-Sommer, Z., and Vandenbussche, M. (2007). A conserved microRNA module exerts homeotic control over *Petunia hybrida* and *Antirrhinum majus* floral organ identity. Nat Genet **39,** 901-905.

Ciaffi, M., Paolacci, A.R., Tanzarella, O.A., and Porceddu, E. (2011). Molecular aspects of flower development in grasses. Sex Plant Reprod **24,** 247- 282.

Clark, S.E., Williams, R.W., and Meyerowitz, E.M. (1997). The *CLAVATA1* gene encodes a putative receptor kinase that controls shoot and floral meristem size in Arabidopsis. Cell **89,** 575-585.

Coen, E.S., and Meyerowitz, E.M. (1991). The war of the whorls: genetic interactions controlling lower development. Nature **353,** 31-37.

Davies, B., Motte, P., Keck, E., Saedler, H., Sommer, H., and Schwarz-Sommer, Z. (1999). *PLENA* and *FARINELLI*: redundancy and regulatory interactions between two *Antirrhinum* MADS-box factors controlling flower development. EMBO J **18,** 4023-4034.

Dreni, L., and Kater, M.M. (2014). MADS reloaded: evolution of the *AGAMOUS* subfamily genes. New Phytol **201,** 717-732.

Dreni, L., Pilatone, A., Yun, D., Erreni, S., Pajoro, A., Caporali, E., Zhang, D., and Kater, M.M. (2011). Functional analysis of all AGAMOUS subfamily members in rice reveals their roles in reproductive organ identity determination and meristem determinacy. Plant Cell **23,** 2850-2863.

Eshed, Y., Baum, S.F., Perea, J.V., and Bowman, J.L. (2001). Establishment of polarity in lateral organs of plants. Current Biology **11,** 1251-1260.

Flanagan, C.A., Hu, Y., and Ma, H. (1996). Specific expression of the *AGL1* MADS-box gene suggests regulatory functions in *Arabidopsis* gynoecium and ovule development. Plant J **10,** 343-353.

Fletcher, J.C., Brand, U., Running, M.P., Simon, R., and Meyerowitz, E.M. (1999). Signaling of cell fate decisions by *CLAVATA3* in *Arabidopsis* shoot meristems. Science **283,** 1911-1914.

Goethe, J.W. (1790). The metamophosis of plants. MIT Press (reprinted in 2009), Cambridge.

Gomez-Mena, C., de Folter, S., Costa, M.M., Angenent, G.C., and Sablowski, R. (2005). Transcriptional program controlled by the floral homeotic gene *AGAMOUS* during early organogenesis. Development **132,** 429-438.

Ha, C.M., Jun, J.H., and Fletcher, J.C. (2010). Shoot Apical Meristem Form and Function. Curr Top Dev Biol **91,** 103-140.

Hiei, Y., Ohta, S., Komari, T., and Kumashiro, T. (1994). Efficient transformation of rice (*Oryza sativa* L.) mediated by *Agrobacterium* and sequence analysis of the boundaries of the T-DNA. Plant J **6,** 271-282.

Hirano, H.-Y., Tanaka, W., and Toriba, T. (2014). Grass flower development. Methods Mol Biol **1110,** 57-84.

Ito, Y., Kimura, F., Hirakata, K., Tsuda, K., Takasugi, T., Eiguchi, M., Nakagawa, K., and Kurata, N. (2011). Fatty acid elongase is required for shoot development in rice. Plant J **66,** 680-688.

Jack, T. (2004). Molecular and genetic mechanisms of floral control. Plant Cell **16 Suppl,** S1-17.

Jessen, D., Roth, C., Wiermer, M., and Fulda, M. (2015). Two activities of long-chain acyl-coenzyme A synthetase are involved in lipid trafficking between the endoplasmic reticulum and the plastid in Arabidopsis. Plant Physiol **167,** 351-366.

Jin, Y., Luo, Q., Tong, H., Wang, A., Cheng, Z., Tang, J., Li, D., Zhao, X., Li, X., Wan, J., Jiao, Y., Chu, C., and Zhu, L. (2011). An AT-hook gene is required for palea formation and floral organ number control in rice. Dev Biol **359,** 277-288.

Keck, E., McSteen, P., Carpenter, R., and Coen, E. (2003). Separation of genetic functions controlling organidentity in ̄owers. EMBO J **22,** 1058-1066.

Kunst, L., and Samuels, L. (2009). Plant cuticles shine: advances in wax biosynthesis

and export. Curr Opin Plant Biol **12,** 721-727.

Kuusk, S., Sohlberg, J.J., Long, J.A., Fridborg, I., and Sundberg, E. (2002). *STY1* and *STY2* promote the formation of apical tissues during *Arabidopsis* gynoecium development. Development **129,** 4707-4717.

Kyozuka, J., Kobayashi, T., Morita, M., and Shimamoto, K. (2000). Spatially and temporally regulated expression of rice MADS box genes with similarity to *Arabidopsis* class A, B and C genes. Plant Cell Physiol **41,** 710-718.

Kyozuka, J., and Shimamoto, K. (2002). Ectopic expression of *OsMADS3*, a rice ortholog of *AGAMOUS*, caused a homeotic transformation of lodicules to stamens in transgenic rice plants. Plant Cell Physiol **43,** 130-135.

Lee, S.B., and Suh, M.C. (2015). Advances in the understanding of cuticular waxes in *Arabidopsis thaliana* and crop species. Plant Cell Rep **34,** 557- 572.

Lenhard, M., Bohnert, A., Jurgens, G., and Laux, T. (2001). Termination of stem cell maintenance in *Arabidopsis* floral meristems by interactions between *WUSCHEL* and *AGAMOUS*. Cell **105,** 805-814.

Li, H., Liang, W., Yin, C., Zhu, L., and Zhang, D. (2011). Genetic interaction of *OsMADS3*, *DROOPING LEAF*, and *OsMADS13* in specifying rice floral organ identities and meristem determinacy. Plant Physiol **156,** 263-274.

Liljegren, S.J., Ditta, G.S., Eshed, Y., Savidge, B., Bowman, J.L., and Yanofsky, M.F. (2000). *SHATTERPROOF* MADS-box genes control seed dispersal in *Arabidopsis*. Nature **404,** 766-770.

Lohmann, J.U., Hong, R.L., Hobe, M., Busch, M.A., Parcy, F., Simon, R., and Weigel, D. (2001). A molecular link between stem cell regulation and floral patterning in *Arabidopsis*. Cell **105,** 793-803.

Lohmann, J.U., and Weigel, D. (2002). Building beauty: the genetic control of floral patterning. Dev Cell **2,** 135-142.

Luo, D., Carpenter, R., Vincent, C., Copsey, L., and Coen, E. (1996). Origin of floral asymmetry in *Antirrhinum*. Nature **383,** 794-799.

Maes, T., Van de Steene, N., Zethof, J., Karimi, M., D'Hauw, M., Mares, G., Van Montagu, M., and Gerats, T. (2001). Petunia *Ap2*-like genes and their role in flower and seed development. Plant Cell **13,** 229-244.

Mikami, M., Toki, S., and Endo, M. (2015). Comparison of CRISPR/Cas9 expression constructs for efficient targeted mutagenesis in rice. Plant Mol Biol **88,** 561-572.

Miyao, A., Iwasaki, Y., Kitano, H., Itoh, J., Maekawa, M., Murata, K., Yatou, O., Nagato, Y., and Hirochika, H. (2007). A large-scale collection of phenotypic data describing an insertional mutant population to facilitate functional analysis of rice genes. Plant Molecular Biology **63,** 625-635.

Miyao, A., Tanaka, K., Murata, K., Sawaki, H., Takeda, S., Abe, K., Shinozuka, Y., Onosato, K., and Hirochika, H. (2003). Target site specificity of the *Tos17* retrotransposon shows a preference for insertion within genes and against insertion in retrotransposon-rich regions of the genome. Plant Cell **15,** 1771-1780.

Mizukami, Y., and Ma, H. (1992). Ectopic expression of the floral homeotic gene *AGAMOUS* in transgenic Arabidopsis plants alters floral organ identity. Cell **71,** 119-131.

Morel, P., Heijmans, K., Ament, K., Chopy, M., Trehin, C., Chambrier, P., Rodrigues Bento, S., Bimbo, A., and Vandenbussche, M. (2018). The Floral C-Lineage Genes Trigger Nectary Development in Petunia and Arabidopsis. Plant Cell **30,** 2020-2037.

Nagasawa, N., Miyoshi, M., Sano, Y., Satoh, H., Hirano, H.-Y., Sakai, H., and Nagato, Y. (2003). *SUPERWOMAN1* and *DROOPING LEAF* genes control floral organ identity in rice. Development **130,** 705-718.

Nobusawa, T., Okushima, Y., Nagata, N., Kojima, M., Sakakibara, H., and Umeda, M. (2013). Synthesis of very-long-chain fatty acids in the epidermis controls plant organ growth by restricting cell proliferation. PLoS Biol **11,** e1001531.

Ohmori, S., Kimizu, M., Sugita, M., Miyao, A., Hirochika, H., Uchida, E., Nagato, Y., and Yoshida, H. (2009). *MOSAIC FLORAL ORGANS1*, an AGL6-like MADS box gene, regulates floral organ identity and meristem fate in rice. Plant Cell **21,** 3008-3025.

Ohmori, Y., Toriba, T., Nakamura, H., Ichikawa, H., and Hirano, H.-Y. (2011). Temporal and spatial regulation of *DROOPING LEAF* gene expression that promotes midrib formation in rice. Plant J **65,** 77-86.

Orashakova, S., Lange, M., Lange, S., Wege, S., and Becker, A. (2009). The *CRABS CLAW* ortholog from California poppy (*Eschscholzia californica*, Papaveraceae), *EcCRC*, is involved in floral meristem termination, gynoecium differentiation and ovule initiation. Plant J **58,** 682-693.

Pinyopich, A., Ditta, G.S., Savidge, B., Liljegren, S.J., Baumann, E., Wisman, E., and Yanofsky, M.F. (2003). Assessing the redundancy of MADS-box genes during carpel and ovule development. Nature **424,** 85-88.

Preston, J.C., and Hileman, L.C. (2009). Developmental genetics of floral symmetry evolution. Trends Plant Sci **14,** 147-154.

Prunet, N., and Jack, T.P. (2014). Flower development in *Arabidopsis*: there is more to it than learning your ABCs. Methods Mol Biol **1110,** 3-33.

Sato, D.-S., Ohmori, Y., Nagashima, H., Toriba, T., and Hirano, H.-Y. (2014). A role for *TRIANGULAR HULL1* in fine-tuning spikelet morphogenesis in rice. Genes Genet Syst **89,** 61-69.

Sato, Y., Hong, S.K., Tagiri, A., Kitano, H., Yamamoto, N., Nagato, Y., and Matsuoka, M. (1996). A rice homeobox gene, *OSH1*, is expressed before organ differentiation in a specific region during early embryogenesis. Proc Natl Acad Sci U S A **93,** 8117-8122.

Satoh, H., Matsusaka, H., and Kumamaru, T. (2010). Use of *N*-methyl-*N*-nitrosourea treatment of fertilized egg cells for saturation mutagenesis of rice. Breeding Sci **60,** 475-485.

Savidge, B., Rounsley, S.D., and Yanofsky, M.F. (1995). Temporal relationship between the transcription of two Arabidopsis MADS box genes and the floral organ identity genes. Plant Cell **7,** 721-733.

Shang, B., Xu, C., Zhang, X., Cao, H., Xin, W., and Hu, Y. (2016). Very-long-chain fatty acids restrict regeneration capacity by confining pericycle competence for callus formation in *Arabidopsis*. Proc Natl Acad Sci U S A **113,** 5101-5106.

Shockey, J.M., Fulda, M.S., and Browse, J.A. (2002). Arabidopsis contains nine long-chain acyl-coenzyme a synthetase genes that participate in fatty acid and glycerolipid metabolism. Plant Physiol **129,** 1710-1722.

Sun, B., Looi, L.-S., Guo, S., He, Z., Gan, E.-S., Huang, J., Xu, Y., Wee, W.-Y., and Ito, T. (2014). Timing mechanism dependent on cell division is invoked by Polycomb eviction in plant stem cells. Science **343,** 1248559.

Sun, B., Xu, Y., Ng, K.-H., and Ito, T. (2009). A timing mechanism for stem cell maintenance and differentiation in the *Arabidopsis* floral meristem. Genes Dev **23,** 1791-1804.

Suzaki, T., Sato, M., Ashikari, M., Miyoshi, M., Nagato, Y., and Hirano, H.-Y. (2004). The gene *FLORAL ORGAN NUMBER1* regulates floral meristem size in rice and encodes a leucine-rich repeat receptor kinase orthologous to *Arabidopsis* CLAVATA1. Development **131,** 5649- 5657.

Suzaki, T., Toriba, T., Fujimoto, M., Tsutsumi, N., Kitano, H., and Hirano, H.-Y. (2006). Conservation and diversification of meristem maintenance mechanism in Oryza sativa: Function of the *FLORAL ORGAN NUMBER2* gene. Plant Cell Physiol **47,** 1591-1602.

Suzuki, T., Eiguchi, M., Kumamaru, T., Satoh, H., Matsusaka, H., Moriguchi, K., Nagato, Y., and Kurata, N. (2008). MNU-induced mutant pools and high performance TILLING enable finding of any gene mutation in rice. Molecular Genetics and Genomics **279,** 213-223.

Tanaka, W., Toriba, T., and Hirano, H.-Y. (2014). Flower development in rice. In The

molecular genetics of floral transition and flower development. F. Fornara, ed 221-262.

Toriba, T., and Hirano, H.-Y. (2014). The *DROOPING LEAF* and *OsETTIN2* genes promote awn development in rice. Plant J **77,** 616-626.

Toriba, T., and Hirano, H.Y. (2018). Two-Color In Situ Hybridization: A Technique for Simultaneous Detection of Transcripts from Different Loci. Methods Mol Biol **1830,** 269-287.

Tsuda, K., Akiba, T., Kimura, F., Ishibashi, M., Moriya, C., Nakagawa, K., Kurata, N., and Ito, Y. (2013). ONION2 fatty acid elongase is required for shoot development in rice. Plant Cell Physiol **54,** 209-217.

Wu, F., Shi, X., Lin, X., Liu, Y., Chong, K., Theissen, G., and Meng, Z. (2017). The ABCs of flower development: mutational analysis of *AP1*/*FUL*-like genes in rice provides evidence for a homeotic (A)-function in grasses. Plant J **89,** 310-324.

Yamaguchi, N., Huang, J., Xu, Y., Tanoi, K., and Ito, T. (2017). Fine-tuning of auxin homeostasis governs the transition from floral stem cell maintenance to gynoecium formation. Nat Commun **8,** 1125.

Yamaguchi, T., Lee, D.Y., Miyao, A., Hirochika, H., An, G., and Hirano, H.-Y. (2006). Functional diversification of the two C-class MADS box genes *OSMADS3* and *OSMADS58* in *Oryza sativa*. Plant Cell **18,** 15-28.

Yamaguchi, T., Nagasawa, N., Kawasaki, S., Matsuoka, M., Nagato, Y., and Hirano, H.-Y. (2004). The *YABBY* gene *DROOPING LEAF* regulates carpel specification and midrib development in *Oryza sativa*. Plant Cell **16,** 500-509.

Yamaki, S., Nagato, Y., Kurata, N., and Nonomura, K.I. (2011). Ovule is a lateral organ finally differentiated from the terminating floral meristem in rice. Dev Biol **351,** 208-216.

Yanofsky, M.F., Ma, H., Bowman, J.L., Drews, G.N., Feldmann, K.A., and Meyerowitz, E.M. (1990). The protein encoded by the *Arabidopsis* homeotic

gene *agamous* resembles transcription factors. Nature **346,** 35-39.

Yao, S.-G., Ohmori, S., Kimizu, M., and Yoshida, H. (2008). Unequal genetic redundancy of rice *PISTILLATA* orthologs, *OsMADS2* and *OsMADS4*, in lodicule and stamen development. Plant Cell Physiol **49,** 853-857.

Yasui, Y., Tanaka, W., Sakamoto, T., Kurata, T., and Hirano, H.-Y. (2017). Genetic Enhancer Analysis Reveals that *FLORAL ORGAN NUMBER2* and *OsMADS3* Co-operatively Regulate Maintenance and Determinacy of the Flower Meristem in Rice. Plant Cell Physiol **58,** 893-903.

Yoshida, A., Suzaki, T., Tanaka, W., and Hirano, H.-Y. (2009). The homeotic gene l ong sterile *lemma* (*G1*) specifies sterile lemma identity in the rice spikelet. Proc Natl Acad Sci U S A **106,** 20103-20108.

Yoshida, H., and Nagato, Y. (2011). Flower development in rice. J Exp Bot **62,** 4719-4730.